A Novel In-Situ Method for Rubidium-Strontium (Rb-Sr) Dating of Igneous Rocks and Minerals

Thesis is submitted in accordance with the requirements of the University of Adelaide for an Honours Degree in Geology

Lise Marie Jensen

October 2017

THE UNIVERSITY of ADELAIDE

A NOVEL IN-SITU METHOD FOR RUBIDIUM-STRONTIUM (Rb-Sr) DATING OF IGNEOUS ROCKS AND MINERALS

RUNNING TITLE

Novel in-situ Rb-Sr dating of igneous rocks and minerals

ABSTRACT

The Rb-Sr isotopic system represents a popular geochronological tool for dating igneous rocks and minerals. This study presents recent advances in the Rb-Sr radiogenic dating via a direct 'in-situ' age determination of biotites based on laser ablation system (LA) coupled with a new generation of triple quadrupole (QQQ) ICP-MS instrument (Agilent 8900). In addition this study also tests (i) the sensitivity and performance of online chemical separation of Rb and Sr in QQQ, using O_2 and N_2O reaction gases, and (ii) the precision and reproducibility of elemental concentrations and $^{87}Sr/^{86}Sr$ data on selected standards with respect to their certified values. Results performed by Agilent 8900 on standard and sample solutions confirmed the reliability and robustness of the chemical separation of Rb and Sr via QQQ where yields of SrO^+ reaction products reach ~12% for O_2 gas, and up to ~99.85% for N_2O gas. The latter was thus applied for the in-situ Rb-Sr dating as well as further tests of Agilent 8900 using rocs standards, which showed that the certified Rb and Sr concentrations in G-2 and GSP-2 granitic standards were reproduced within 2%, and their $^{87}Sr/^{86}Sr$ rations measured by QQQ with N_2O gas agree with the first 4 decimal places with respect to certified values and/or our TIMS measurements.

The acquired in-situ Rb-Sr isochrons ages of biotites from the studied rocks (including granite, gabbro, gneiss) and mineral separates (LP-6 standard) showed a good agreement with the published crystallisation ages for these samples.

Specifically LP-6 yielded an in-situ Rb-Sr age of 127±12 Ma (published whole rock Rb-Sr and K-Ar age of 128.2±2.2 Ma); Padthaway Granite yielded 479.4±9.4 Ma (published U-Pb age of 487.1±1.2 Ma); Black Hill Gabbro yielded 481.6±6 Ma (published whole rock Rb-Sr and K-Ar age of 487±5 Ma); and finally Rathjen Gneiss was dated at 502.0±9.9 Ma (published U-Pb and Rb-Sr age of 514±5 Ma). Overall, this study and the above in-situ Rb-Sr ages of biotites confirmed the potential and robustness of the LA-QQQ system (i.e. Agilent 8900 with N_2O gas) for geochronology applications, such as direct dating of biotite-bearing igneous and metamorphic rocks.

KEYWORDS

Geochronology, In-situ Rb-Sr Dating, Igneous Rocks, Minerals, Agilent 8900 LA-QQQ

TABLE OF CONTENTS

LIST OF FIGURES AND TABLES

1. INTRODUCTION

Historically thermal ionization mass spectrometry (TIMS), coupled with isotope dilution method, was used to determine accurately the concentrations of Rb and Sr, as well as $^{87}Sr/^{86}Sr$ and $^{87}Rb/^{86}Sr$ ratios, which in turn provide absolute age determinations for igneous minerals and rocks via a Rb-Sr isochrons dating and geochronology. This well-established method involved a lengthy process of offline chemical separation of Sr from Rb by column chemistry, and precise gravimetric calibrations of the isotope spikes. The TIMS method has obtain precise measurements of the isotopic $^{87}Sr/^{86}Sr$ ratios, but this method is not able to simultaneously measure also $^{87}Rb/^{86}Sr$ ratios, as Rb and Sr need to be separated and analysed independently by TIMS approach. This is due to an isobaric interference of ^{87}Rb on ^{87}Sr, which is also due to a beta-decay of ^{87}Rb to ^{87}Sr.

With the recent refinements of the ^{87}Rb λ decay constant $1.3972\pm0.0045\ 10^{-11}$ yr (Villa, De Bièvre, Holden, & Renne, 2015) and new technological advancements, there has been interest in establishing a new dating method for Rb-Sr isotopic system to gain reliability with precision and accuracy of the absolute Rb-Sr dating of minerals and rocks (see Zack and Hogmalm (2016). The latter study takes advantage of a newly developed triple quadrupole (QQQ) technology coupled with a laser ablation system (LA) and analytical instrumentation such as Agilent ICP-MS. Agilent Technologies had released in 2012 their first triple quadrupole ICP-MS (ICP-QQQ) system (Agilent 8800), followed by a more sensitive and advanced model (Agilent 8900), which was used for the Rb-Sr dating presented in this study. This system incorporates the concept of two quadrupoles positioned on either side of the gas collision/reaction cell (CRC) (Figure 1), allowing for isotopic ions to be targeted in the first quadrupole (Q1), that go through the CRC, and all other ions are excluded from entering the CRC; the targeted ions will react with a reaction gas and be mass-shifted, then pass into the second quadrupole (Q2) to be detected by the detector.

The mass-shift mode and type of reaction gas used are a couple of key elements to overcome any isobaric interferences that occurs during isotope analysis of Rb and Sr on mass 87, due to the same *m*/*z* ratios for isotopes of ^{87}Rb and ^{87}Sr present in the sample and standards.

The pioneering works of Bolea-Fernandez, Balcaen, Resano, and Vanhaecke (2016) have tested the online separation of Sr from Rb (via ICP-QQQ) using the CH_3F/He reaction gas, to conduct accurate determination of $^{87}Sr/^{86}Sr$ isotopic ratios in natural samples. Recently Bolea-Fernandez et al. (2016) also tested the precision and accuracy of $^{87}Sr/^{86}Sr$ analysis with laser ablation coupled with the Agilent 8800 ICP-QQQ (LA-ICP-MS/MS) for rocks with high $^{87}Rb/^{86}Sr$ ratios by using CH_3F/He as the reaction gases in wet and dry plasma conditions. Finally Zack and Hogmalm (2016) also experimented with laser ablation for Rb-Sr dating with the online separation method for extracting ^{87}Sr from ^{87}Rb using O_2 as a reaction gas; and Hogmalm, Zack, Karlsson, Sjöqvist, and Garbe-Schönberg (2017) generated the first coupled K-Ca and Rb-Sr in-situ dating of micas with LA-ICP-MS/MS using N_2O and SF_6 as reaction gases. The aim of this study is to follow up on some of these new developments for Rb-Sr dating based on the ICP-QQQ technology, and continue to explore the Rb-Sr dating method using the latest model of Agilent 8900 ICP-QQQ (Figure 2) together with more reactive O_2 and N_2O gases for the online separation of Rb and Sr.

1.1. Project aims

This study aims to accomplish the following tasks using the Agilent 8900 ICP-QQQ

- Task 1: Investigate the reliability, precision and accuracy of the new Agilent 8900 ICP-QQQ in comparison to TIMS data, by testing with solution for Rb and Sr concentrations and $^{87}Sr/^{86}Sr$ ratios on samples of known aged granitic rocks with K-bearing mineral.

- Task 2: Investigate the production and yields of the reaction products of Sr isotopes from O_2 and N_2O gases on the Agilent 8900 ICP-QQQ.
- Task 3: Test and compare the newly developed in-situ Rb-Sr dating method on selected K-bearing and Rb-rich granitic minerals and rocks with known published ages, the latter determined by other well-established isotope dating techniques such as U-Pb, Rb-Sr and K-Ar.

The above research tasks are designed to test the robustness and reliability of the new Agilent 8900 ICP-QQQ for the Rb-Sr dating method, and evaluate its potential and limitations for the applications in geochronology and earth sciences.

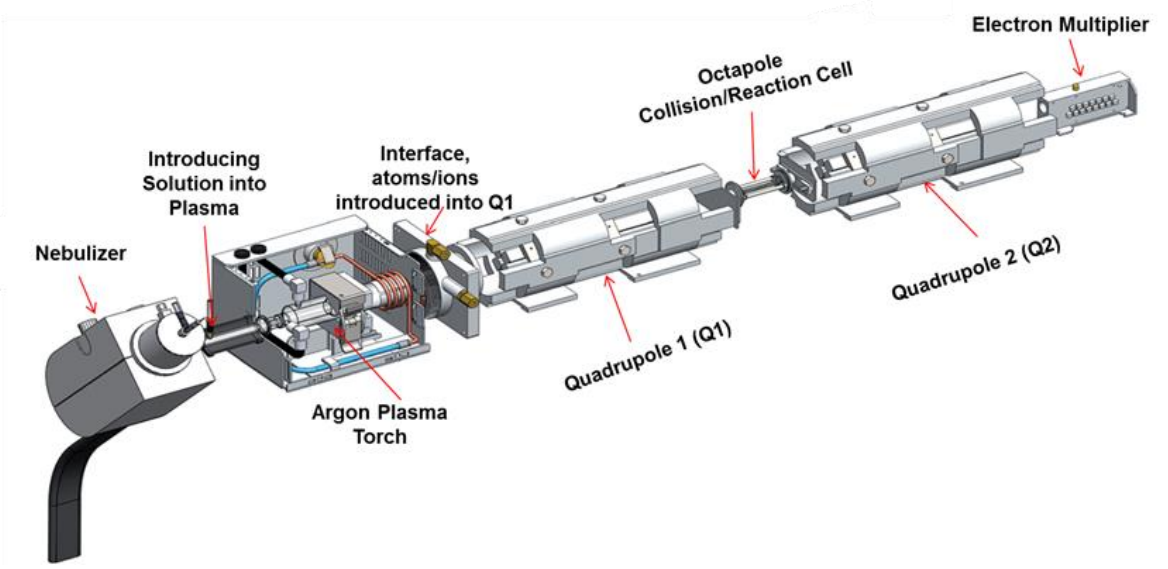

Figure 1: The quadrupole set-up within the Agilent 8800/8900 series of the ICP-QQQ (Bolea-Fernandez, Balcaen, Resano, & Vanhaecke, 2017).

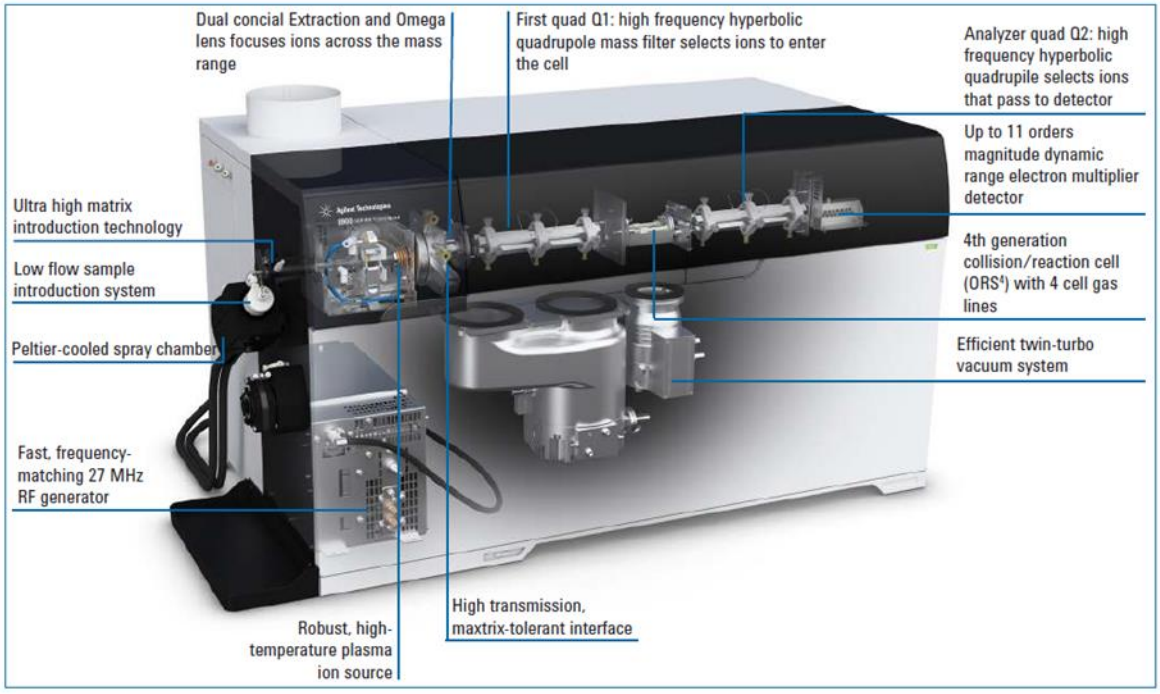

Figure 2: Features of the new Agilent 8900 ICP-QQQ, (Technologies, 2016).

2. REGIONAL GEOLOGICAL SETTING WITH RELEVANCE TO STUDY SAMPLES

Samples of minerals and rocks selected for this study originates from igneous and metamorphic rocks exposed in Southern Australia (SA), (Figure 5). These samples comprise of (i) granites, (ii) gneisses, and (iii) gabbro, which are part of the southern region of SA, was formed during a tectonic convergence of the Ross-Delamerian Orogen. The corresponding magnitude of stress occurred from the eastern edge of Gondwana, had transferred to the southeastern edge of Australia (Foden, Elburg, Dougherty-Page, & Burtt, 2006), which is reflected as the transition from passive margin (i.e. Precambrian to Early Cambrian sediments) to a compressional deformation and simultaneous development of granitic intrusions forming the Adelaide Fold Belt (Figure 5), including the studied samples (i.e. Padthaway Granite, Rathjen Gneiss and Black Hill Gabbro). Overall, this meta-igneous region extends about 1100 km to the north from Peak and to western tip of Kangaroo Island in the south (Foden et al., 2006). The three rock samples investigated in this study have emplacement or crystallisation published by Foden et al. (2006), Foden, Sandiford, Dougherty-Page, and Williams (1999), and Milnes, Compston, and Daily (1977) and the available geochemical and isotope analyses also constrains the sources and origins of magma for the formation of these rocks. Specifically, the Rathjen Gneiss is chemically associated with I-Type granitic rock formed during the Delamerian Orogen. In contrast, Padthaway Granite shows affinities to A-Type granitic rocks that were formed post-tectonically (Foden et al., 1999), and the latter origin is also suggested for Black Hill Gabbro.

The geochronological history of Adelaide Fold Belt had been originally described and reconstructed by Compston, Crawford, and Bofinger (1966), and later refined by Milnes et al. (1977), based on the K-Ar and Rb-Sr geochronology. More recently Foden et al. (2006) further constrained the commencement and termination timing of the Delamerian Orogen event by high-precision U-Pb dating of zircons.

The results indicate the Delamerian Orogen had begun around ~514±4 Ma and ended at ~490±3 Ma (Foden et al., 2006). Based on these published results, the established duration of the Delamerian Orogeny was on the order of about 24 ± 4 Ma (Figure 6). The relatively abrupt termination of this orogenic event is related to further tectonic processes such as rapid uplift, followed by cooling and the onset of an extension (Foden et al., 2006).

2.1. Rock and mineral samples

The three rock samples: Rathjen Gneiss, Black Hill Gabbro and Padthaway Granite have known published ages (Foden et al. (2006), Foden et al. (1999), and Milnes et al. (1977) or Table 22) and these will be compared in this study to the newly acquired Rb-Sr ages determined via the LA-QQQ method using Agilent 8900 ICP-QQQ. In addition the comparison of our laser ablation (LA) in-situ Rb-Sr dating with the published U-Pb and K-Ar ages on identical rocks will allow for possible interpretations in terms of common crystallisation ages and/or the impacts of different closing temperatures on the above isotopes systems due to younger metamorphic events.

2.1.1 Rathjen Gneiss (RG)

A granitic-granodiorite of medium-to-coarse grained orthognessis, located north of Palmer latitude 34.45, longitude 139.08, (Foden, Elburg, et al., 2002), with geochemically indicating an I-type granite (Foden et al., 1999). Rock matrix consists of feldspars of plagioclase partially zoned, potassium feldspar (microcline) mildly perthitic, quartz, hornblende and biotite; and is characterised by gneissic foliations (Foden et al., 1999) minerals observed from the thin section in Figure 3.

Rathjen Gneiss is found in the central core of the Delamerian orogeny, placed within the highest metamorphic grade (Foden et al., 1999). This rock had been formed in a syntectonic setting; whereby the commencement of deformation with the advent of magmatic granitic intrusion had been synchronised forming the Adelaide Thrust-Fold Belt. (Foden et al., 2006).

Foden et al. (1999) dated the Rathjen Gneiss to 514±4 Ma using U-Pb dating method (Figure 6), which constrains the magmatic emplacement age of the granitic intrusion and the onset of the tectonic convergence of the Delamerian Orogen forming the Adelaide Thrust-Fold Belt.

2.1.2 Black Hill Gabbro (BHG-1)

A coarse grained monzogabbro, located in Cambria, West Murray Valley which lies 90 km ENE of Adelaide latitude 34.41, longitude 139.28, with a geochemical signature indicates an A-type granite (Foden, Elburg, et al., 2002). The matrix comprises of subhedral to anhedral perthitic alkali feldspar, plagioclase, quartz, hornblende and biotite (Milnes et al. (1977) and (Turner, 1996). Original petrological analysis of Black Hill gabbronic complex was discussed by Turner (1996) and not included in this work. The Black Hill gabbronic pluton had intruded the Adelaide Fold Belt after the termination of the Delamerian Orogeny (Turner & Foden, 1996). The initial work of Milnes et al. (1977) had dated the Black Hill Gabbro to 487±5 Ma by K-Ar dating method (Figure 6) that indicates the intrusion had occurred post-tectonically which suggests the timing of the emplacement of the intrusion was after Delamerian Orogeny had ceased. This age has been confirmed by the work of Turner (1996) by the Rb-Sr and Sm-Nd dating methods gave an age of 489±39 Ma, in which had been corrected to 487 Ma.

2.1.3 Padthaway Granite (PG-11)

A homogeneous coarsely-crystalline granitic rock with characteristic interlocking texture and pink colour when weathered, but the appearance is green for unweathered samples. Located in Coonawarra, south-eastern of South Australia latitude 35.45, longitude 139.30 (Foden, Elburg, et al., 2002), were formed post-tectonic of the Delamerian Orogeny and does not display metamorphic fabrics (Turner, Foden, & Morrison, 1992). The matrix comprises of microcline feldspar, plagioclase, smoky quartz, biotite and hornblende (Turner et al., 1992); illustrated in the thin section in Figure 4. The mineralogy, geochemical and isotopic signature is of the A-type granite that shows the Padthaway Ridge rocks had evolved through fractionation from parent basaltic magma (Turner et al., 1992). The work of Foden et al. (2006) had constrained the intrusion emplacement age of Padthaway Granite to 487.1±1.2 Ma by the U-Pb dating method (Figure 6)

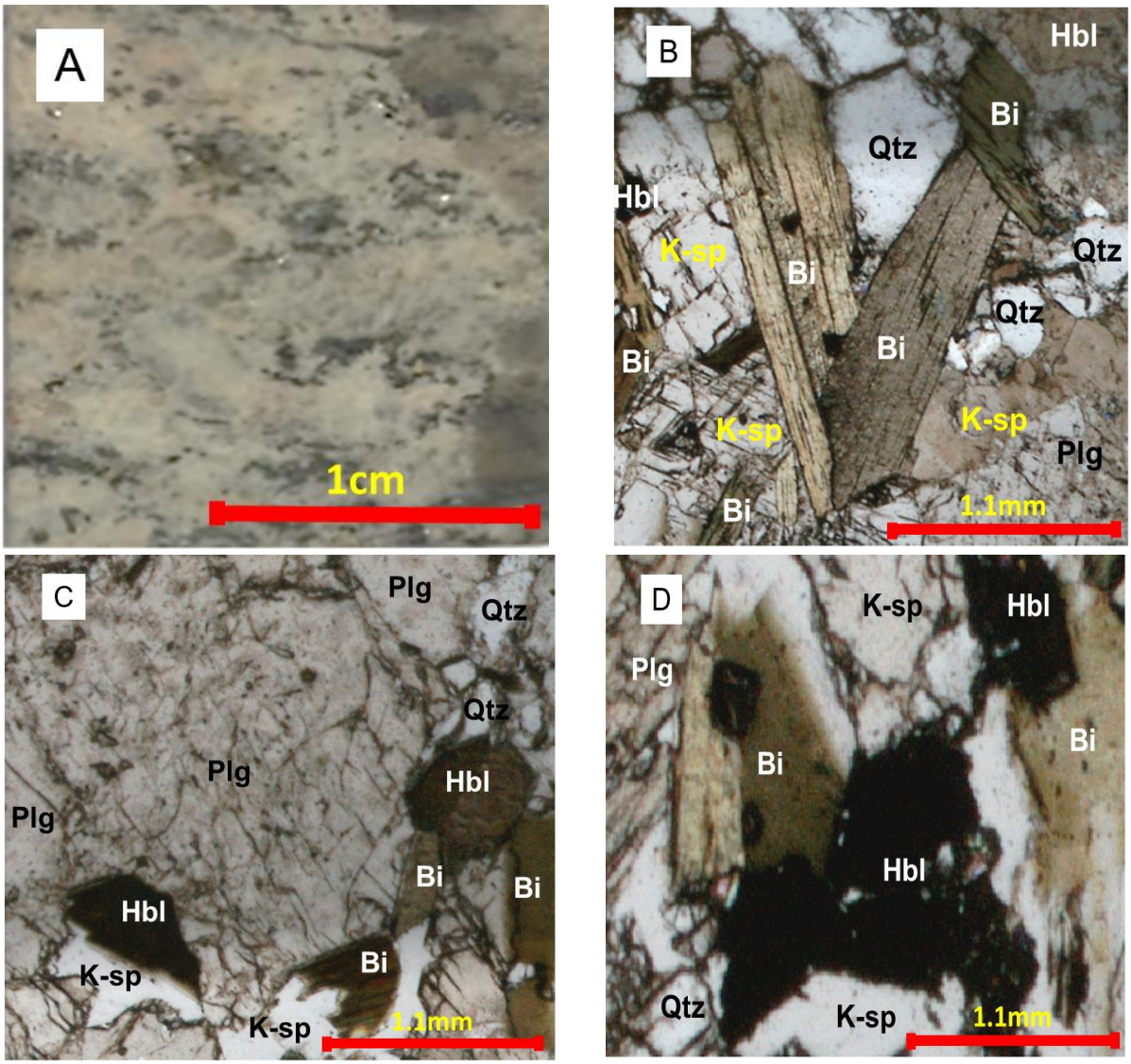

Figure 3: Sample of Rathjen Gneiss (RG).
A. RG rock piece ~2cm x ~1.5cm, orthogneiss showing compositional gnessic foliation of layered pinkish and white feldspars mixed with quartz, and blackish platy layers of hornblende and biotite; B. Biotite brownish-green to brown elongated grains with inclusions, boarded by K-feldspar, quartz, plagioclase and hornblende; C. Slight perthitic plagioclase bordered by small grains of hornblende, biotite, quartz and K-feldspar; D. Hornblende grain with biotite grains alongside with an inclusion, boarded by K-feldspar and quartz grain and slight perthitic plagioclase.

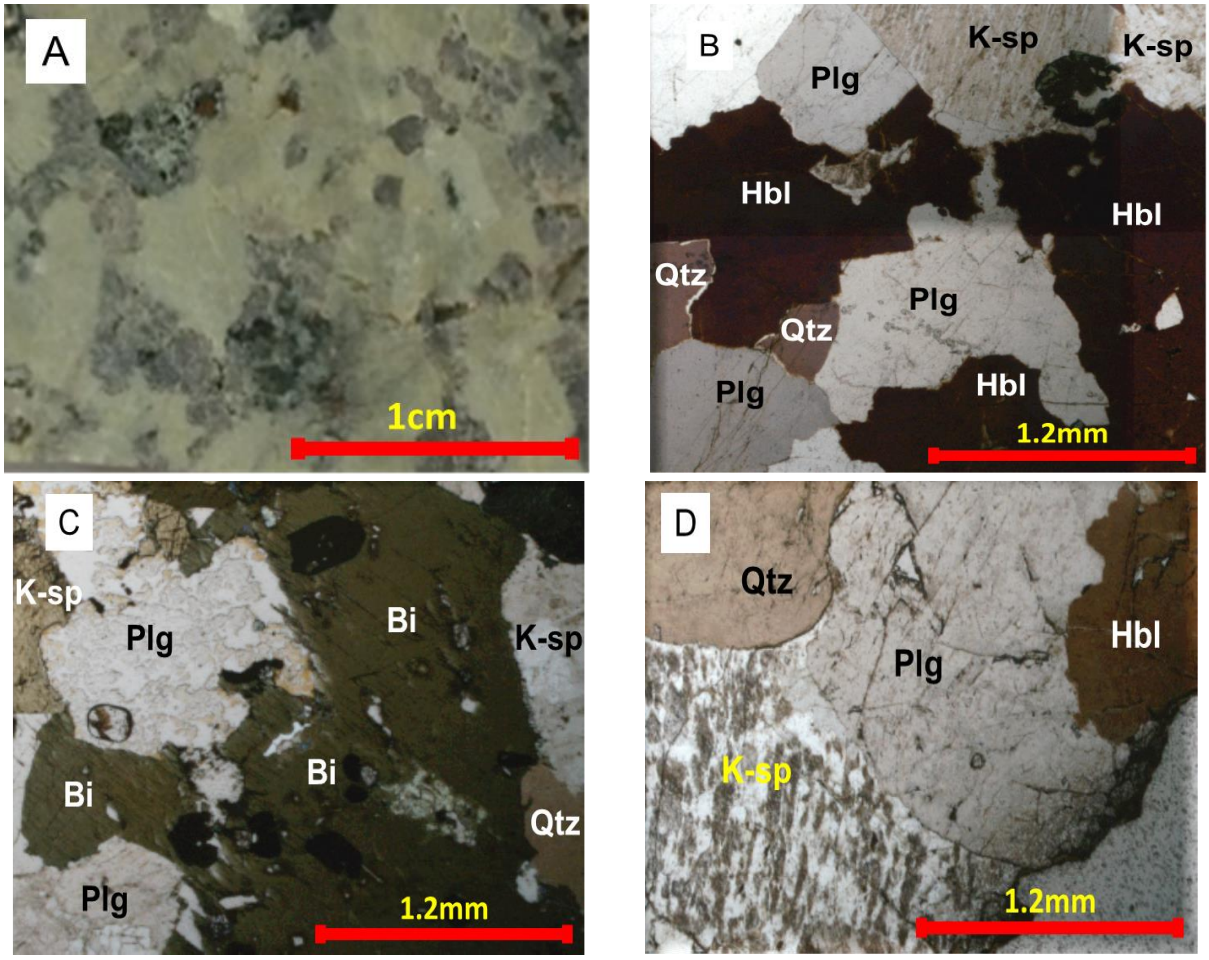

Figure 4: Sample of Padthaway Granite (PG-11).
A. PG-11 rock piece ~2cm x ~2cm with phaneritic interlocking texture of coarse-grains including green microcline feldspar, plagioclase, quartz and dark grains of hornblende and biotite; B. Individual interlocking grains of plagioclase encircled by hornblende and quartz grains that are bordered with plagioclase and microcline feldspar; C. Biotite brownish-green grains bordered by plagioclase, quartz and K-feldspar; D. Individual interlocking grains of quartz, microcline feldspar, plagioclase and hornblende.

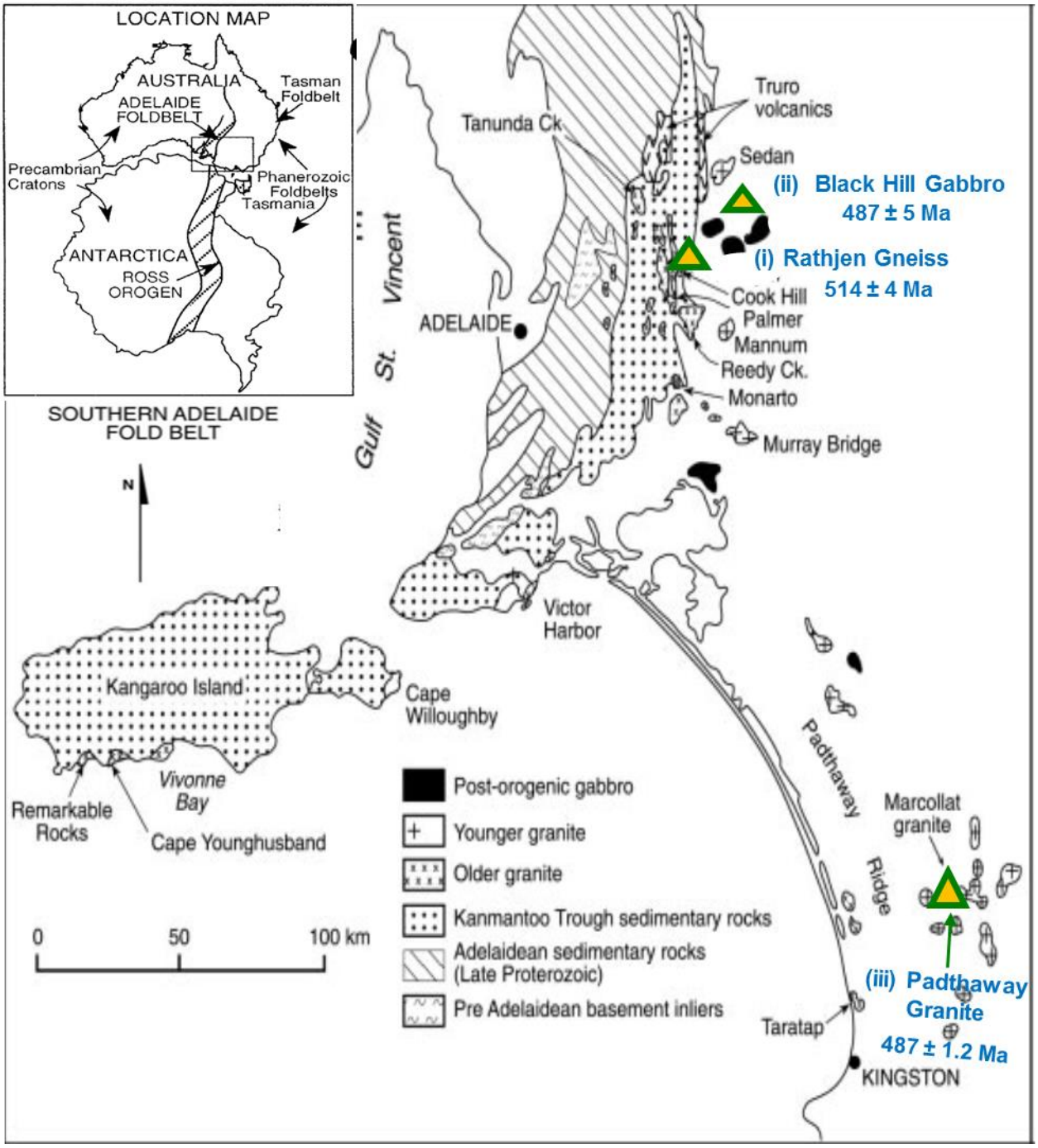

Figure 5: Map of Southern Adelaide Fold Belt.
Insert pre-Australian-Antarctic breakup of Ross-Delamerian Orogen (Foden, Song, et al., 2002); and locations of the studied rock samples and ages (i.e triangles) within the Southern Adelaide Fold Belt, including (i) Rathjen Gneiss, (ii) Black Hill Gabbro and (iii) Padthaway Granite (modified map from Foden et al. (1999).

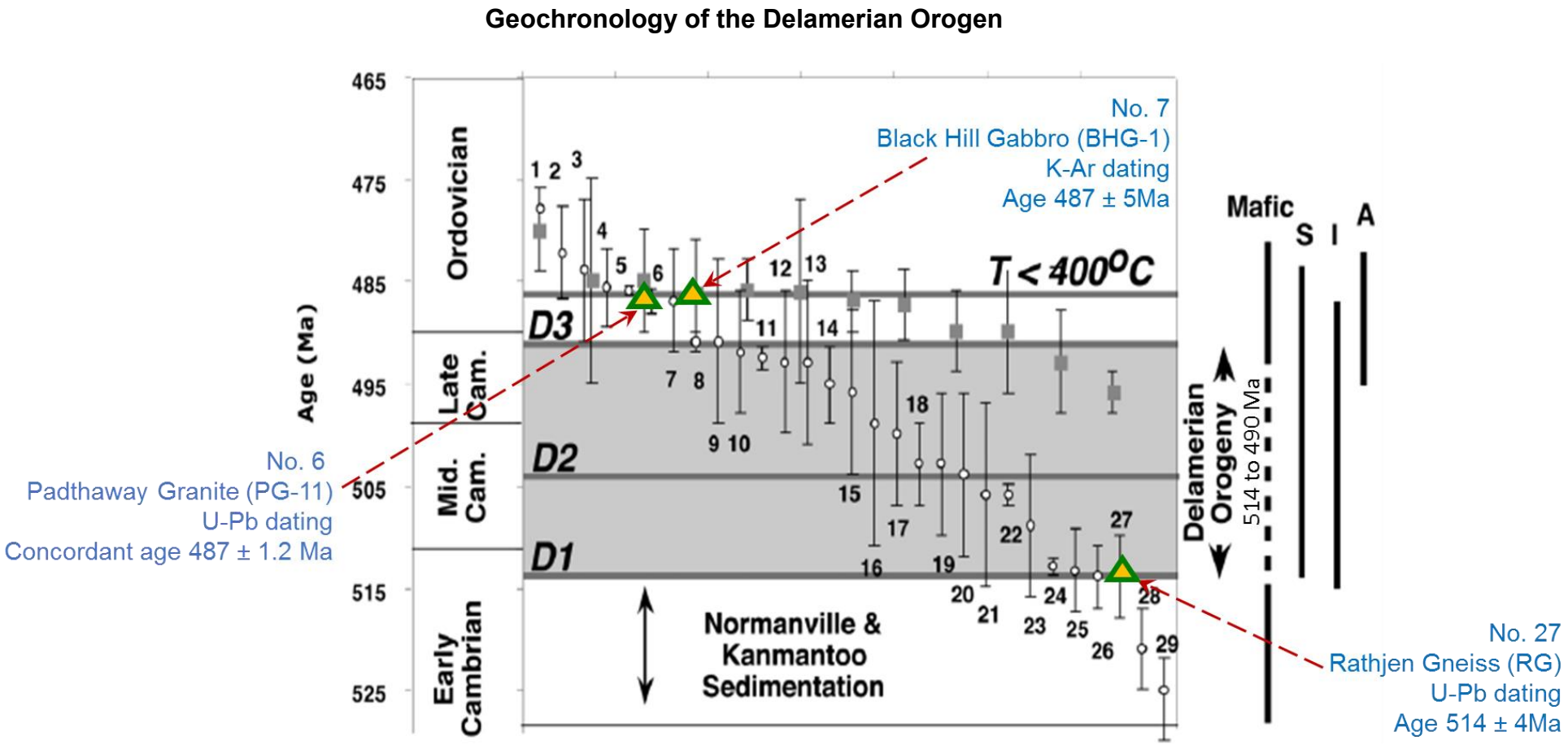

Figure 6: Schematic geochronology of the Delamerian Orogen with time periods of rock formations, emplacement age and dating methods (modified from Foden et al. (2006), including also the samples investigated in this study.

2.2. Standards

For the purposes of data calibration and quality control of the solution-based analysis using ICP-QQQ, this study also investigated a set of certified geological standards. These include (i) a pure elemental Sr isotope standard (NIST SRM 987), (ii) USGS rock standards (G-2, GSP-2), and (iii) a mineral-separate standard composed of biotite (LP-6). These different standards and their geochemical properties relevant to the Rb-Sr system, are described in detail below.

2.2.1 Solution standards (prepared from homogeneous powders)

- NIST SRM 987 (Strontium Carbonate), for matrix matching to the stock solution of Strontium (Sr) 10 µg/mL High Purity Standard, abundance ratios: $^{88}Sr/^{86}Sr = 8.37861 \pm 0.00325$, $^{87}Sr/^{86}Sr = 0.71034 \pm 0.00026$
- USGS G-2 (Granite), recommended values: Rb = 170 µg/g, Sr = 478µg/g, abundance ratio $^{87}Sr/^{86}Sr = 0.70983$
- USGS GSP-2 (Granodiorite), recommended values Rb = 245 µg/g, Sr = 240 µg/g, abundance ratio $^{87}Sr/^{86}Sr = 0.764962$
- *LP-6 (Biotite), calculated values from geochoronometry equation 5, (this work: concentration Rb = 273.8 ppm, Sr = 18.4 ppm, $^{87}Rb/^{86}Sr = 50.9$, $^{87}Sr/^{86}Sr = 0.80371$), age 128.2±2.2 Ma, initial $^{87}Sr/^{86}Sr = 0.7130 \pm 0.0014$. (Li, Chen, Li, Wang, & He, 2008) has low radiogenic ^{87}Sr.

  *Note: LP-6 was also used for laser ablation as a standard.

2.2.2 Laser standards

For the LA-based QQQ analysis for the Rb-Sr isotope system, we employed a set of well characterised standards comprising either glasses (NIST SRM 610 and 612) or pressed nano-powder standards of mineral separates (i.e. Mica-Mg) provided to us by Prof. Thomas Zack from University of Gothenburg. More details on the standards used for LA-QQQ are listed below.

Supplied by Adelaide Microscopy, University of Adelaide

- NIST SRM 610 (Glass) recommended values Rb = 425.7 mg/kg±0.8, Sr = 515.5 mg/kg ±0.5, abundance ratio $^{87}Rb/^{86}Sr$ = 2.33, abundance ratio $^{87}Sr/^{86}Sr$ = 0.7094±0.0002
- NIST SRM 612 (Glass) recommended values Rb = 31.4 mg/kg ± 0.4, Sr = 78.4 mg/kg ±0.2; abundance ratio $^{87}Sr/^{86}Sr$ = 0.7089±0.0002
- USGS BCR-2G (Basalt) recommended values Rb = 48 µg/g±2, Sr = 346 µg/g±14, abundance ratio $^{87}Rb/^{86}Sr$ = 0.3901 abundance ratio $^{87}Sr/^{86}Sr$ = 0.704958

Supplied by Thomas Zack, University of Gothenburg

- Mica-Mg (Phlogopite) recommended values Rb = 1300 µg/g, Sr = 27 µg/g (Govindaraju, 1994) Rb-Sr age 495±15 Ma (Govindaraju, 1979) as pressed nano-powders (Zack & Hogmalm, 2016).

3. METHODOLOGY AND ANALYTICAL EXPERIMENTS TESTED WITH ICP-QQQ

The newly installed Agilent 8900 ICP-QQQ at Adelaide Microscopy, University of Adelaide is currently dedicated for solution work and determination of elemental concentrations. In this section we describe several experiments performed on ICP-QQQ in order to test the capabilities and limits of the ICP-QQQ system for the measurements of Rb and Sr elemental concentrations and isotope compositions, using both solution-based and LA approaches. These experiments are outlined in Table 1; and the Flowchart 1 in Figure 7 also illustrates a schematic overview for these different experiments.

In addition, other methods outlined in this section include: petrographic studies; preparation of elemental standards; preparation of rock samples: acid digestion and dilution; dilution of standards and samples; laser mount preparation; instrument calibrations; analytical procedure and conditions. (See Appendix 7)

Table 1: List of experiments

No of experiments	Solution/Laser	No. samples	Testing	Anticipated outcome
Experiment 1	Diluted solutions of Rb, Sr and Rb-Sr mixed with varying ppb concentrations	3 Standards 4 Samples	• O_2 gas reaction products • Concentration	• Reaction products of Sr isotopes • No reaction products for Rb • Good concentrations for Rb and Sr
Experiment 2	Diluted solutions of Rb, Sr and Rb-Sr mixed with varying ppb concentrations	3 Standards 4 Samples	• N_2O gas reaction products • Concentration • Ratio	• Reaction products of Sr isotopes • No reaction products for Rb • Good concentrations for Rb and Sr • Good $^{87}Sr/^{86}Sr$ ratios
Experiment 3 (a & b)	Laser mounts of whole rock and biotite mineral	5 Standards 4 Samples	• In-situ dating method with laser	• Similar ages to published ages of rock and mineral samples
Experiment 4	Dissolved whole rock powders and biotite minerals diluted in solution	3 Standards 4 Samples	• Concentrations	• Good concentrations for Rb and Sr from published data

Note: Experiment 3 was conducted in two parts (a and b) over two days.

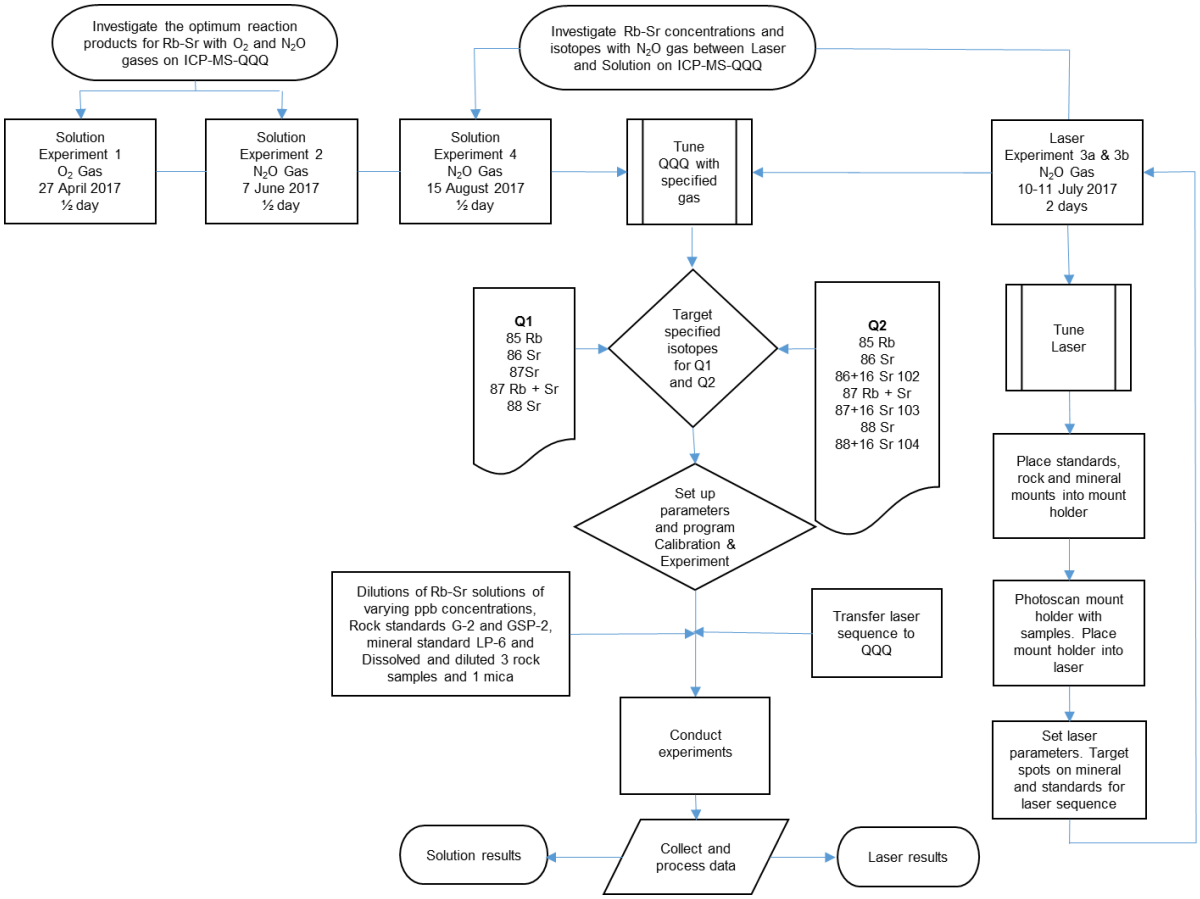

Figure 7: Flowchart 1– Overview of experiment flow conducted on Agilent 8900 ICP-QQQ.

3.1. Petrography and optical microscopy

Samples of Rathjen Gneiss and Padthaway Granite rocks were prepared for thin sections, which were then viewed and examined using a Nikon, optical petrographic microscope equipped with a digital camera on 2.5 mm x magnification at Adelaide Microscopy. Scanned stitched images were made of both thin sections. Mineral identification of the thin sections was performed following the optical properties outlined by Perkins & Henke (2004).

3.2. Preparation of elemental standards

All solution preparations were conducted in the Clean Laboratory, Mawson building, University of Adelaide. Solutions were prepared specifically for online separation of Rb and Sr, testing on the new Agilent 8900 ICP-QQQ for the analysis of optimum reactions of O_2 gas in Experiment 1 and N_2O in Experiment 2 and the same solutions were used for Experiment 4 for the calibration curve. Stock solution was used to prepare and mix: (2%) .320M Nitric Acid (HNO_3); Rubidium (Rb) 10 µg/mL High Purity Standard and Strontium (Sr) 10 µg/mL High Purity Standard in three stages. Four reference standards were used for solution work: SRM 987, G-2, GSP-2 and LP-6. All vials, rock powders, mineral separates and solutions were weighed on the Mettler Toledo AT201 series scale to 5^{th} decimal place, and small amounts of solutions were measured by using 1 ml and 5 ml pipettes. (see Appendix 1, 2 and 3)

3.3. Preparation of rock samples: acid digestion and dilution for ICP-QQQ analysis

Cutting and crushing of rocks and mineral samples were conducted at the Rock Preparation Facility, Mawson building, University of Adelaide. Rock samples were cut to size: 1) RG: ~2 cm x ~1.5 cm; and 2) PG-11: ~2 cm x ~2 cm, on the Gemmasta lathe. Cleaning procedure of Ring mill: with appropriate safety equipment, clean the mill and mill head with some quartz gravel (to clean off any residual of previous rock), crushing into powder, remove bulk of the quartz powder, and clean the remainder of quartz powder with compressed air gun, then using ethanol wipe inside and pulverisers; clean bench top with ethanol of any rock powder before crushing samples. This cleaning procedure was completed before crushing the next sample.

Placed one of the two samples to be crushed using the Rocklabs Bench Top Ring Mill, into the mill head TC200-27084 using 5cm diameter mill head, (~80 g) crushing rock for ~5 minutes into very fine powder. Testing after ~2 minutes for fineness of powder; to gage the fineness, feel for any rough particles. Rock powder is placed onto clean piece of paper then transferred into plastic lock bag and labelled appropriately. RG sample weighed ~14 g and PG-11 sample weighed ~26 g. BHG-1 rock powder had been crushed into powder prior to this study (see Appendix 4 rock digestion)

3.4. Dilution of standards and samples

The whole rock powder in bombs and mineral separates in vials were completely dissolved (Appendix 4). A dry yellowish-orange residual powder settled on the bottom of bombs and vials. The rock residual powder was diluted using Equation 1 (Appendix 6). The two stages outlined below:

Stage 1: Dry residual powders in bombs and vials, diluted 10x 10 ml (for LP-6 20 ml dilute 10x) of HNO_3; shake with care to dislodge all dry residual powders from bottom of vials; this solution is transferred to 20 ml vials.

Stage 2: ~39.6 ml HNO_3 into Sarstedt 50 ml vials; pipette 0.4ml 10x diluted dissolved rock and mineral samples, using clean pipette tip for each sample and weight in between measurements. The concentrations were converted from ppm to ppb during the dilution process.

The dilution factors and acid volumes applied are listed in the Appendix 5.

3.5. Preparation of mounts for LA-QQQ

The preparation of five laser mounts from mineral separates and rocks are outlined below in two steps: microscope and mounts; and for lapidary process see Appendix 12.

3.7.1 Microscope

The microscopes used for this method were Olympus SZ61, located in the Microscope room, Mawson building, University of Adelaide.

Step 1: Mineral separates of the two biotite's sized between ~50-100 µm were placed on separate white paper; the mineral grains viewed under one microscope, and handpicked using metallic pick; under another microscope the mineral grains on the metallic pick were placed carefully on double sided tape, one side stuck to the base of mould for the mount (25 mm).

3.7.2 Mounts

The three biotite's and two whole rock (RG and PG-11) mounts are ready for EpoxiCure 2: 100 parts Resin: 23 parts Hardener. The measurement by weight ratio for one standard 25 mm mount requires 5 g:1.15 g of Resin and Hardener.

Step 2 Prepare moulds for mounts, spraying a thin layer of releasing agent; using digital scales weigh and pour into a small plastic beaker 5 g of Epoxy Resin then weigh and add 1.15 g of Epoxy Hardener; stir with stick to mix together the resin and hardener making sure no air bubbles occur; pour ready mixture into moulds; 6 hours for cuing time.

3.6. Instrument tuning and calibration

For the development of the Rb-Sr isotope dating method the Agilent 8900 ICP-QQQ instrument for both solution-based work and laser ablation, the internal standard tuning was performed using (i) O_2 reaction gas in the collision/reaction cell for experiment 1; and (ii) N_2O reaction gas for experiments 2, 3 and 4. Each parameter (Table 3) was adjusted utilising the interface software within the Agilent 8900 ICP-QQQ for optimising the instrument conditions for experimentation. The reference standards used for calibration curves are shown in Table 2 used to evaluate and adjust for the accuracy and precision of samples.

Table 2: Reference standards used for solution and laser calibration curves

Experiments	1	2	3		4
Test mode	Solution	Solution	Laser		Solution
Reference standards	• 2 blank HNO_3 • Rb-Sr 10ppb • RB-Sr 20ppb • Rb-Sr 50ppb • Rb-Sr 100ppb	• 2 blank HNO_3 • Rb-Sr 10ppb • RB-Sr 20ppb • Rb-Sr 50ppb • Rb-Sr 100ppb • Rb-Sr 250ppb • Rb-Sr 500ppb • Blank HNO_3	*3a • SRM 610 • SRM 612 • BCR-2G • Mica Mg A4 (3 spots 74µm)	*3b • SRM 610 • SRM 612 • BCR-2G • Mica Mg A4 • Muscovite C1 (2 spots 74µm)	• 2 blank HNO_3 • Rb-Sr 20ppb • Rb-Sr 50ppb • Rb-Sr 100ppb • Rb-Sr 250ppb • Rb-Sr 500ppb • Blank HNO_3
*over 2 days					

3.7. Analytical procedures and software used for ICP-QQQ data and age determinations

The analytical procedures and data processing used in this study for the Rb-Sr isotope dating are as follows: Excel, Isoplot and Glitter programs, plus the instrument conditions for O_2 and N_2O reaction gases for solution and LA-based analysis are shown in Table 3.

3.9.1 Excel

Prior to solution experiments 1, 2 and 4, calculations of dilution factors were calculated in Excel (see Appendix 2, 3, 5 and 6). The raw data for all experiments from the Agilent 8900 ICP-QQQ were exported into Excel 2013 and manipulated by reducing the data in a more manageable format for calculations to occur.

Equations used to calculate the reaction products of O_2 and N_2O are shown in Appendix 6. Briefly, the following variables were measured and/or calculated: ^{88}Sr and ^{104}SrO; Rb and Sr concentrations of standards and samples; and $^{87}Sr/^{86}Sr$ ratios of G-2 and GSP-2 standards; and $^{87}Rb/^{86}Sr$ for LP-6 biotite standard. These variables, specifically the corrected $^{87}Sr/^{86}Sr$ and $^{87}Rb/^{86}Sr$ ratios, were then used to calculate the *isochron* ages using Isoplot software available as add-in in Excel (see below for details).

3.9.2 Isoplot

Isoplot 4.15 was used for the calculation of 'ages' for the analysed minerals and rocks based on the radiogenic Rb-Sr isotope system, and this software was also used for a graphical presentation of the measured data (i.e. normalised and corrected Excel data) in a classical 'isochron' plot with $^{87}Sr/^{86}Sr$ versus $^{87}Rb/^{86}Sr$ coordinates. For the age calculations presented in this study the correction factor applied to all samples for $^{87}Rb/^{86}Sr$ ratio of 0.02 and $^{87}Sr/^{86}Sr$ ratio 0.01 and the updated decay constant (λ) for the Rb-Sr system of $1.3972\pm0.0045 \times 10^{-11}$ yr (Villa et al., 2015) was used and applied in Isoplot.

3.9.3 Glitter

Glitter 4.4.4 software (Macquarie University) was used to process the LA-QQQ data including (i) the removal of background signal, and (ii) selection of intervals with rubust signals from the analysed minerals (i.e. sample ablation signals – see Appendix 14). The process used for background signal reduction of laser ablation was by selecting the pixelmap colour brightness signal for the targeted isotopes: ^{85}Rb, ^{87}Rb, ^{88}Sr, ^{87}Sr and ^{86}Sr to find the best signal. From the 'Review window', the signal line for each sample was corrected by smoothing out spikes where possible. The reduced laser data was transferred to Excel.

3.9.4 Agilent 8900 ICP-QQQ conditions

All solution and laser experiments were conducted and analysed at Adelaide Microscopy, University of Adelaide, with Agilent 8900 ICP-QQQ. The following plasma conditions were used: RF power laser 1350W, Ar carrier gas flow rate 1.00 L/min; RF power solution 1550W, Ar carrier gas flow rate 1.09 L/min with a Micro Mist nebuliser and Scott Type spray chamber. Collision cell in He mode 1.0 mL/min gas flow for ^{85}Rb, ^{87}Rb, ^{86}Sr, ^{87}Sr, ^{88}Sr, in O_2 40% flow rate and N_2O 33% flow rate for Sr measuring reaction mode for SrO^+ reaction products (i.e.$^{88}Sr^+ \rightarrow {}^{88}Sr^{16}O$ measured at mass 104; $^{87}Sr^+ \rightarrow {}^{87}Sr^{16}O$ measured at mass 103; and $^{86}Sr^+ \rightarrow {}^{86}Sr^{16}O$ measured at mass 102). The online internal standard element of normalisation with respect to indium (In) was used to correct and monitor any drifts in signals and/or ionisation efficiencies. The instrument conditions for both O_2 and N_2O solution work and N_2O laser ablation are also summarised in Table 3.

Table 3: Experiment parameter settings on Agilent 8900 ICP-QQQ for solution and laser

Parameter	Units	Experiment 1 O_2 MS/MS Rb-Sr	Experiment 2 & 4 N_2O MS/MS Rb-Sr	Experiment 3a Laser N_2O MS/MS Rb-Sr	Experiment 3b Laser N_2O MS/MS Rb-Sr
ICP					
Plasma					
RF power	W	1550	1550	1350	1350
RF matching	V	1.80	1.80	1.20	1.20
Sample depth	mm	8.0	8.0	3.5	3.5
Carrier gas	L/min	1.09	1.09	1.00	1.00
Nebulizer pump	rps	0.10	0.10	0.00	0.00
S/C temp	°C	2	2	2	2
Gas switch		Makeup gas	Dilution gas	Makeup gas	Makeup gas
Lenses					
Extract 1	V	-2.0	-2.0	-9.0	-9.0
Extract 2	V	-165.0	-165.0	-250.0	-250.0
Omega bias	V	-80	-80	-150	-130
Omega lens	V	7.0	7.0	5.5	5.5
Q1 entrance	V	-5	-5	-5	-5
Q1 exit	V	-1	-1	1	1
Cell focus	V	3.0	3.0	3.0	3.0
Cell entrance	V	-110	-80	-80	-80
Cell exit	V	-150	-150	-150	-150
Deflect	V	-5.0	-10.0	-10.0	-10.0
Plate bias	V	-110	-110	-110	-90
Q1					
Q1 mass gain		126	126	126	126
Q1 mass offset		125	125	125	125
Q1 axis gain		0.9998	0.9998	0.9998	0.9998
Q1 axis offset		-0.04	-0.04	-0.04	-0.04
Q1 bias	V	0.0	0.0	0.0	-4.0
Q1 Prefilter bias	V	-10.0	-10.0	-10.0	-10.0
Q1 Postfilter bias	V	-7.0	-7.0	-7.0	-26.0
Cell					
He flow	mL/min	0.0	1.0	1.0	0.0
H_2 flow	mL/min	0.0	1.0	0.0	0.0
3rd gas flow	%	0	10	5	0
4th gas flow	%	40	0	0	33
OctP bias	V	-25.0	-25.0	-25.0	-25.0
Axial acceleration	V	2.0	2.0	2.0	2.0
OctP RF	V	180	180	180	180
Energy discrimination	V	-10.0	-10.0	-14.0	-14.0
Torch Axis					
Torch H	mm	0.3	0.3	-	-
Torch V	mm	0.0	0.0	-	-
EM					
Discriminator	mV	3.6	3.6	-	-
Analog HV	V	2183	2183	-	-
Pulse HV	V	1029	1029	-	-
Meters					
IF/BK press	Pa	1.44E+2	1.39E+2	1.66E+2	1.54E+2
Analyzer press	Pa	1.45E-3	2.67E-3	-	-
Water RF/WC/IF	L/min	-	-	1.19	1.19
Internal temp	°C	36.5	37.9	39.0	38.4
Carrier gas (BP)	kPa		3.67E+2	-	-
Inlet Temp	°C	-	-	31.4	31.1
Reflected power	W	3	2	2	1
Forward power	W	1551	-	-	-

3.9.5 Laser ablation (LA) running conditions

The Agilent 8900 ICP-QQQ was coupled with the ASI RESOlution ArF 193µm excimer laser ablation (LA) system (see Appendix 15) with a large format S150 sample chamber (Appendix 13), held at Adelaide Microscopy, University of Adelaide. The ICP-MS-QQQ coupled with the laser allowed for further advances to new in-situ Rb-Sr dating technique, modified after Bolea-Fernandez et al. (2016), Zack and Hogmalm (2016), and Hogmalm et al. (2017), to measure directly the $^{87}Sr/^{86}Sr$ and $^{87}Rb/^{86}Sr$ ratios in feldspar and mica minerals. The samples had an ablated spot size of 74µm, a fluence of ~3.5 J/cm^2 with a repetition rate of 5Hz; in a He atmosphere (0.35 L/min flow rate) and transported to the Agilent 8900 ICP-QQQ with a mixed aerosol of Ar carrier gas (1.06 L/min flow rate). For each analysis there was 22s of background gas and 42s of ablation signal as the laser was firing. The primary standard for drift and mass-bias correction was NIST SRM 610, and the secondary standard NIST SRM 612 for analysis. The Agilent 8900 ICP-QQQ collision/reaction cell operated in reaction mode using N_2O gas (total 5% flow). Isotopes measured on-mass: ^{85}Rb, ^{87}Rb, ^{86}Sr, ^{87}Sr and ^{88}Sr; and mass-shifted reaction products $Sr^+ + N_2O \rightarrow Sr^{16}O^+ + N_2$: $^{86}Sr \rightarrow {}^{102}Sr$, $^{87}Sr \rightarrow {}^{103}Sr$ and $^{88}Sr \rightarrow {}^{104}Sr$. Count times for each isotope was 0.01-0.05 seconds with a total sweep time of 0.362 seconds.

4. RESULTS

For all experiments conducted the equations applied to calculate the results are listed in Appendix 6.

4.1. Experiment 1

Experiment 1 links to Tasks 1 and 2 (see section 1.1 Project aims) which aims to test the robustness and reliability of O_2 reaction gas for the measurements of Sr isotopes in solution, specifically investigating the precision and accuracy of the measured $^{87}Sr/^{86}Sr$ ratios relative to certified elemental and rock standards. Part of the experiment was monitoring instrument drift on the Agilent 8900 ICP-QQQ, reaction product yields, and reproducibility of the measured Sr concentrations and $^{87}Sr/^{86}Sr$ ratios. Optimum tuning parameters for the highest acquired yields for the reactions of Sr^+ to SrO^+ with O_2 gas are listed in Table 3. Figure 8 illustrates O_2 instrument drift, and was corrected by using the equation from Bolea-Fernandez et al. (2016) for internal and external corrections to improve the results of Sr 100 ppb solution to 0.701427±0.0061. The standards used for this experiment are listed in Table 4. Reaction products are seen in Table 5 were calculated using Equation 3 from raw data of each sample using ^{88}Sr and mass-shifted ^{104}SrO. The results show 87% of ^{88}Sr did not react and 12% of ^{104}SrO had reaction products in mass-shift mode. Table 6 indicates the results of Rb and Sr concentrations, which were calculate using Equation 2. The standards show that G-2 ^{85}Rb had a deviation of -8.4%, and ^{104}SrO a deviation of -4.8% and for GSP-2 ^{85}Rb had a deviation of -10.1% and ^{104}SrO a deviation of -0.8% from the recommended values. The $^{87}Sr/^{86}Sr$ ratios in Table 7, were calculated using Equation 4. The standards $^{87}Sr/^{86}Sr$ ratios for G-2 had a deviation of 0.4186% and GSP-2 a negative deviation of -0.4169%, from recommended TIMS values. (For experiment design see Appendix 8)

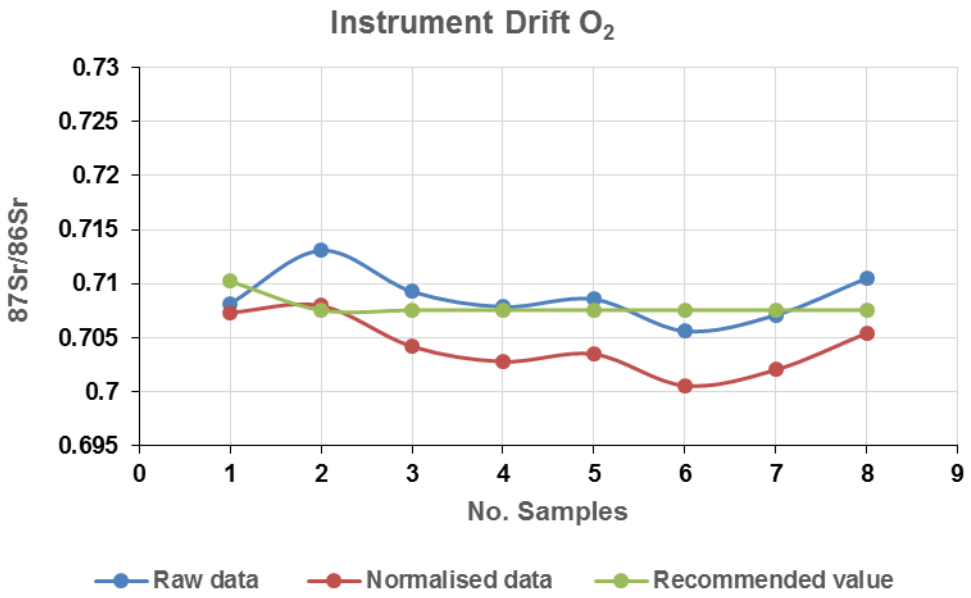

Figure 8: O_2 instrument drift.

The equation used to correct instrument drift from Bolea-Fernandez et al. (2016) paper.

Table 4: O_2 solution standards

Standard	Recommended $^{87}Sr/^{86}Sr$	Correction Factor
Sr ppm	0.707571	1.001177
G-2	0.709748	1.007207
GSP 2	0.76511	1.003008
SRM 987	0.710246	0.997078

The correction factors for each standard were calculated using Equation 4.

Table 5: O_2 reaction products

Sample	Counts Per Second		Total CPS	Reaction Products	
*n=1, **n=2	^{88}Sr	^{104}Sr		^{88}Sr	^{104}Sr
G-2*	4573471.237	627470.677	5200942	87%	12%
GSP-2*	2285394.034	309345.442	2594739	88%	11%
SRM 987*	479644.195	65653.781	545298	87%	12%
Sr 100**	948118.642	129853.68	1077972	87%	12%

The reaction products for each sample were calculated using Equation 3.

Table 6: O_2 concentrations for Rb and Sr

Sample	^{85}Rb ppm	Recommended	Deviation (%)
G-2	154.3	168.5± 3	-8.4
GSP-2	220.2	245 ± 7	-10.1
	^{104}Sr ppm		
G-2	464.2	474.9 ± 2	-4.8
GSP-2	235.9	240 ± 10	-0.8

The concentrations for each standard were calculated using Equation 2.

Table 7: O_2 ratio of $^{87}Sr/^{86}Sr$

Sample n=1	QQQ ^{103}Sr/^{102}Sr	Normalised	Recommended ^{87}Sr/^{86}Sr	*Normalisation factor	Deviation %
G-2	.714863 ± 0.0003	**.712719**	.709748 ± 2	1.003008	0.4186
GSP-2	.767411 ± 0.0004	**.76192**	.765120 ± 2	1.007270	-0.4169

The $^{87}Sr/^{86}Sr$ ratios for the standards were calculated using Equation 4.

Note: *GSP-2 correction factor (1.003008) from Table 4 was used to calculate G-2 normalised value and vice versa for GSP-2.

4.2. Experiment 2

Experiment 2 links to Tasks 1 and 2 which tested the robustness and reliability for Sr concentration and isotope analysis using N_2O reaction gas in solution, with the same investigation as per Experiment 1 for the measured $^{87}Sr/^{86}Sr$ ratios relative to certified elemental and rock standards. The tuning conditions for N_2O gas in Table 3. The observed instrument drift (see Figure 9) showed only very limited drift using N_2O gas and thus no internal correction was applied. The standards used for this experiment are listed in Table 8. The reaction products are listed in Table 9 calculated using Equation 3 from raw data of each sample. Overall the results show 0.15% of ^{88}Sr did not react with N_2O gas and 99.85% of ^{104}SrO had reaction products in mass-shift mode. Table 10 indicates the results of Rb and Sr concentrations which were calculated using Equation 2. The standards show that for G-2 sample (i.e. granitic rock standard) the measured Rb concentrations deviate from certified values within about -1.7%, and for Sr concentration the deviation is about 0.1%. For GSP-2 (granitic rock standard) the deviation for Rb is -0.7% and for Sr -0.5% from recommended values (see Table 10). The measured and corrected $^{87}Sr/^{86}Sr$ ratios are listed in Table 11, calculated using Equation 4 and our reported $^{87}Sr/^{86}Sr$ ratios for G-2 deviate within 0.0235 (% deviation) from the certified values and for GSP-2 the deviation is -0.0235%, from the recommended TIMS values. (For experiment design see Appendix 8)

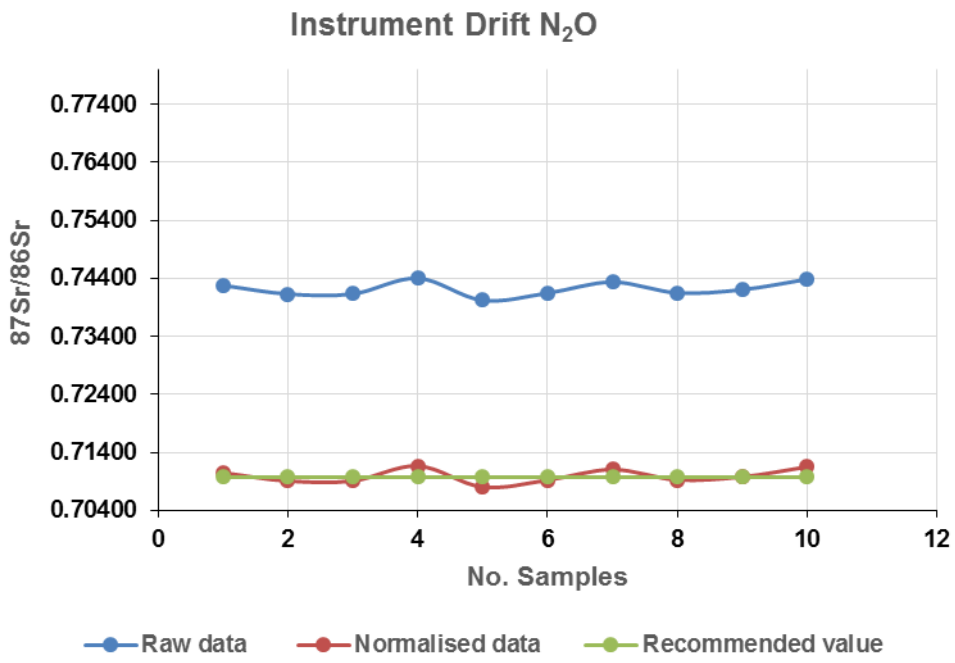

Figure 9: N_2O instrument drift.

Table 8: N_2O solution standards

Standard	Recommended $^{87}Sr/^{86}Sr$	Correction Factor
Sr ppm	0.707571	1.016259
G-2	0.709748	1.045704
GSP-2	0.76511	1.045458
SRM 987	0.710246	1.016471

The correction factors for each standard were calculated using Equation 4.

Table 9: N_2O reaction products

Sample	CPS		Total CPS	Reaction Products	
*n=10, **n=6, ***n=12	^{88}Sr	^{104}Sr		^{88}Sr	^{104}Sr
G-2*	79793.71	53917521.45	53997315.16	0.15%	99.85%
GSP-2*	38423.583	26094406.17	26132829.76	0.15%	99.85%
SRM 987**	9001.148	6013021.704	6022022.852	0.15%	99.85%
Sr 100***	18135.759	12217803.71	12235939.47	0.15%	99.85%

The reaction products for each sample were calculated using Equation 3.

Table 10: N_2O concentrations for Rb and Sr

Sample	^{85}Rb ppm	Recommended	Deviation (%)
G-2	165.59 ±0.5	168.5± 3	-1.7
GSP-2	245.25 ± 0.4	245 ± 7	0.1
	^{104}Sr ppm		
G-2	466.6 ±0.5	474.9 ± 2	-1.7
GSP-2	238 ±0.4	240 ± 10	-0.5

The concentrations for each standard were calculated using Equation 2.

Table 11: N_2O ratios of $^{87}Sr/^{86}Sr$

Sample n=10	QQQ ^{103}Sr/^{102}Sr	Normalised	Recommended ^{87}Sr/^{86}Sr	*Normalisation factor	Deviation %
G-2	.74219 ± 0.0003	**.709915**	.709748 ±2	1.045458	0.0235
GSP-2	.79989 ± 0.0004	**.76493**	.765120 ± 2	1.045704	-0.0235

The ^{87}Sr/^{86}Sr ratios for the standards were calculated using Equation 4.

Note: *GSP-2 correction factor (1.045458) from Table 8 was used to calculate G-2 normalised value and vice versa for GSP-2.

4.3. Experiment 3

Experiment 3 links to Task 3 which aims to apply in-situ Rb-Sr dating method using LA-QQQ setup. The laser had targeted biotite minerals within whole rocks of Rathjen Gneiss (RG) and Padthaway Granite (PG-11) and biotite mineral separates of Black Hill Gabbro (BHG-1), and LP-6 (see Table 3 for LA-QQQ conditions and Appendix 13 for mount setup). The ratios of the unknown rock and mineral samples (Table 12) were corrected using data acquired from LP-6 and Mica-Mg biotite standards. Table 14 lists the acquired Rb-Sr ages of the samples analysed, which were corrected using the average from Mica-Mg and LP-6 $^{87}Rb/^{86}Sr$ and $^{87}Sr/^{86}Sr$ ratios listed in Table 12. Overall, applying the above approach the reported in-situ Rb-Sr ages of the studied rocks and mineral separates were well-constrained and close to the published ages (see also data Figure 12). The individual Rb-Sr isochron ages for our studied samples, acquired by LA-QQ, are shown in Figure 10. Specifically LP-6 shows spread of data that plot on the isochron line, however with rather large error bars for the $^{87}Sr/^{86}Sr$ ratio, which is due to limited variations of radiogenic ^{87}Sr ingrowth in LP-6 ($^{87}Sr/^{86}Sr$ ranges only from ~0.78 to ~0.86) as a consequence of its young age and relatively lower Rb content; b) PG-11 shows an evenly spread samples starting with small error bars on the isochron but as ^{87}Rb is decreasing the error bars become wider; c) BHG-1 shows a clustering of samples with small error bars on the x axis from 80 to 120 $^{87}Rb/^{86}Sr$ ratio and one approximately at 180 with large $^{87}Rb/^{86}Sr$ ratio error indicating a decrease of ^{87}Rb within the sample; d) RG shows the sample cluster higher up the isochron with small error for $^{87}Sr/^{86}Sr$ ratio and large variations in $^{87}Rb/^{86}Sr$ ratios. (For experiment design see Appendix 11)

Table 12: Laser standards

	$^{87}Rb/^{86}Sr$			$^{87}Sr/^{86}Sr$	
Standard	**Recommended**	**Correction Factor**	**Standard**	**Recommended**	**Correction Factor**
NIST 610	2.331	2.334	NIST 610	0.7097	1.028
NIST 612	1.130	2.201	NIST 612	0.7091	1.028
BCR-2G	0.390	2.341	BCR-2G	0.7050	1.029
Mica-Mg	154.6	2.771	Mica-Mg	1.8525	1.027
LP-6	50.9	2.572	LP-6	0.80371	1.043
Average		2.672			1.035

The correction factors for each standard were calculated using Equation 4.

At the time of this experiment LP-6 biotite was not used as a standard as the elemental Rb and Sr abundances in LP-6 were not known or previously reported in the literature (but see Li et al. (2008). This was overcome by using the results from Experiment 4 (i.e. solution work on LP-6) and measured concentrations of Rb = 273.8 ppm and Sr = 18.4 ppm in LP-6. Rearranging the geochoronometry equation (Equation 5) to calculate the $^{87}Rb/^{86}Sr$ ratio = 50.9 and $^{87}Sr/^{86}Sr$ ratio = 0.80371 in LP-6 biotite standard.

Table 13: In-situ $^{87}Rb/^{86}Sr$ and $^{87}Sr/^{86}Sr$ ratio results

Sample	**Experiment 3 In-situ Rb-Sr**	
All Biotite	$^{87}Rb/^{86}Sr$	$^{87}Sr/^{86}Sr$
LP-6	50.860	0.803711
BHG-1	1.916	1.7310
PG-11	196.731	84.9599
RG	40.518	17.8333
Corrected to averages: LP-6 and Mica-Mg standards		

The $^{87}Rb/^{86}Sr$ and $^{87}Sr/^{86}Sr$ ratios for the samples were calculated using Equation 4.

Table 14: In-situ Rb-Sr dating ages

Sample	Age (Ma)	Initial $^{87}Sr/^{86}Sr$	MSWD
LP-6 Biotite	127 ± 12	0.7201 ± 0.0067	0.56
Padthaway Granite (PG-11) Biotiite	479.4 ± 9.4	0.7200 ± 0.0071	0.43
Black Hill Gabbro (BHG-1) Biotite	481.6 ± 9.6	0.7202 ± 0.0070	0.55
Rathjen Gneiss (RG) Biotite	502.0 ± 9.9	0.7100 ± 0.0071	0.57

The correction factors applied to the ratios $^{87}Rb/^{86}Sr$ is 0.02 and $^{87}Sr/^{86}Sr$ 0.01 for all isochrons.

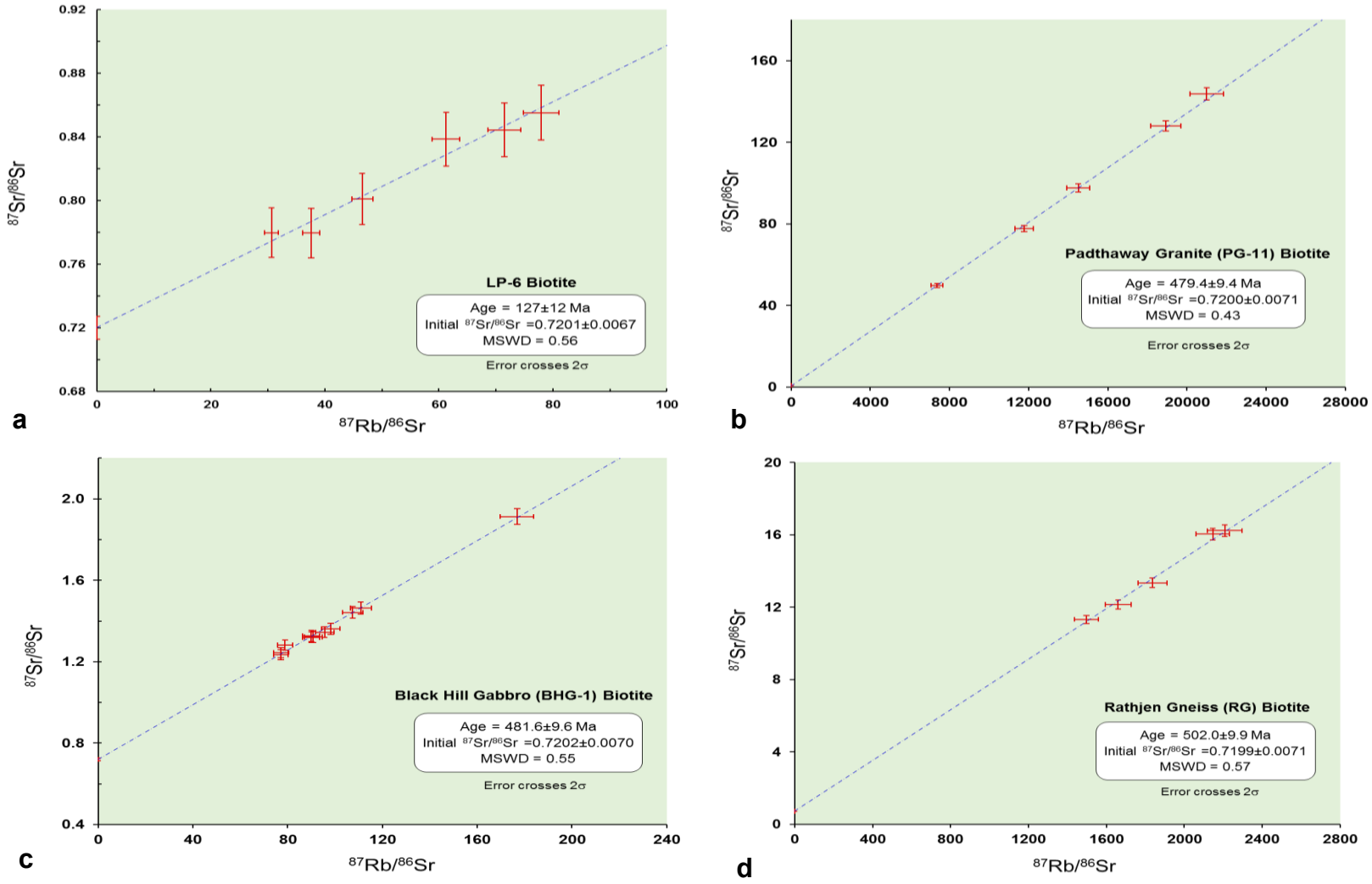

Figure 10: In-situ Rb-Sr isochrons of a: LP-6, b: PG-11, c: BHG-1, d: RG.

4.4. Experiment 4

Experiment 4 links to Task 1 which was testing reliability and the accuracy of the measured Sr and Rb concentrations (and $^{87}Rb/^{86}Sr$ and $^{87}Sr/^{86}Sr$ ratios) for G-2 and GSP-2 standards determined in solution, and their comparison to certified values. Part of this task was also determination of the concentrations of Rb and Sr in the whole rocks of RG, BHG-1 and PG-11; and BHG-1 biotite and LP-6 biotite. Table 16 and Table 17 are the results for concentrations of elemental, rock standards and rock samples, which were calculated using Equation 2 from the standards in Table 15. These results confirmed that the measured concentrations of G-2 deviates by 2.9% for Rb, and 1.8% for Sr; and for GSP-2 the measured Rb concentrations deviates by 1.9%, and for Sr by 1.6% from the recommended values.

Table 15: Solution standards

$^{87}Rb/^{86}Sr$			$^{87}Sr/^{86}Sr$		
Standard	**Recommended**	**Correction Factor**	**Standard**	**Recommended**	**Correction Factor**
G-2	1.003404	2.6639	G-2	0.70975	1.010291
GSP-2	2.881318	2.67077	GSP-2	0.76512	1.010850
LP-6	50.8607	1.94172	LP-6	0.80371	1.01067
Sr 40			Sr 40	.707571	1.012678
Average		2.667333			1.011122

The correction factors for each standard were calculated using Equation 4

Table 16: Concentrations of Rb and Sr (in ppm) for standards

	Concentrations		
Sample	**Published**	**Experiment 4 N_2O**	**Deviation %**
G-2			
Rb ppm	168.5± 3	173.5 ± 0.28	2.9
Sr ppm	474.9 ± 2	483.7± 0.74	1.8
GSP-2			
Rb ppm	245 ± 7	249.7± 0.40	1.9
Sr ppm	240 ± 10	243.9±0.36	1.6

The concentrations for each standard were calculated using Equation 2

Table 17: Concentrations of Rb and Sr (in ppm) for samples

Experiment 4 N_2O	
Sample	**Concentrations**
Padthaway Granite (PG-11)	
Rb ppm	99.8 ± 0.069
Sr ppm	121.7 ±0.017
Black Hill Gabbro (BHG-1)	
Rb ppm	71.3 ± 0.15
Sr ppm	558.9 ± 0.95
Black Hill Gabbro (BHG-1) Biotite	
Rb ppm	502.2 ±0.54
Sr ppm	29.5 ± 0.02
Rathjen Gneiss (RG)	
Rb ppm	109.3 ± 0.06
Sr ppm	109.3 ± 0.06

The concentrations for each standard were calculated using Equation 2

5. DISCUSSION

5.1. O_2 and N_2O gases

Oxygen (O_2) as a reactive gas has been proven by other studies by Bandura, Baranov, and Tanner (2001), Zack and Hogmalm (2016) that it does effectively remove polyatomic and doubly charged interferences when in mass-shift mode (Zack & Hogmalm, 2016). As for this study O_2 gas was initially used, as the laboratory was only equipped with this gas. The first experiment tested Rb and Sr solutions using online separation, with targeted Rb and Sr isotopes in mass-shift mode, to obtain as many counts per second of reaction products, to gain a sense of concentrations of Rb and Sr, $^{87}Sr/^{86}Sr$ ratios. At a later stage of the project, the laboratory had acquired also more reactive N_2O gas with which the second experiment had been conducted with the same intentions as the previous experiment using O_2 gas and Rb and Sr solutions. Results of instrument drift monitored via measured, $^{87}Sr/^{86}Sr$ for O_2 gas are available in Figure 8 and for N_2O gas in Figure 9, illustrating the relative sensitivity of precision of $^{87}Sr/^{86}Sr$ ratios using these two approaches. Overall, the N_2O gas is far more sensitive and yielded smaller precision on $^{87}Sr/^{86}Sr$ ratios of about ±0.0003 (on rock G-2 standard), while measurements with O_2 gas show relatively larger error of ±0.0061.

The yield or reaction products of Sr in mass-shift mode between O_2 and N_2O (Table 18) gases were significantly different. The differences have also been reflected in the works by Hogmalm et al. (2017) on the Agilent 8800 ICP-QQQ with laser. The reaction products that Hogmalm et al. (2017) had obtained using Sr^+ (SrO^+) in mass-shift mode for O_2 gas was 10% with 90% non-reactive products and for N_2O gas was 85% with 15% non-reactive products. However, in this study the reaction products for Sr^+ (SrO^+) in mass-shift mode for O_2 gas was 12% with 88% non-reactive products and for N_2O gas it was 99.85% which was obtained in both solution and laser, only leaving 0.15% of Sr as non-reactive products (Table 18).

Thus this study indicates the overall improvements of sensitivity within the instrument by an increase of 14.85% of reaction products for N_2O gas in mass-shifted mode for Sr^+ isotopes.

The precision of concentrations of Rb and Sr; and the $^{87}Sr/^{86}Sr$ ratios measurements for the rock standards G-2 and GSP-2 in solution work had improved significantly as the experiments progressed (Experiments 1, 2 and 4). The results of each were compared with the TIMS recommended values of concentrations and $^{87}Sr/^{86}Sr$ ratios. For O_2 gas based experiments, the standards yielded the concentrations of Rb and Sr (Table 21) that had large negative deviations while the $^{87}Sr/^{86}Sr$ ratios (Table 19) were more reproducible with smaller deviations. Importantly, for N_2O gas experiments, the concentrations of Rb and Sr (Table 21) as well as the $^{87}Sr/^{86}Sr$ ratios (Table 19) were both reproduced well with respect to recommended values, and had significantly smaller deviations compared to our results from O_2 experiments. The good precision and accuracy achieved was evident for $^{87}Sr/^{86}Sr$ ratios measured with N_2O gas, as these data agree with the first 4 decimal places to TIMS recommended values (Table 20).

Table 18: Reaction efficiency between O_2 and N_2O gases

Reaction Efficiency of Sr Isotopes				
Laser** ****Solution** ** Laser and Solution**	**O_2 Gas**		**N_2O Gas**	
	Reactive products	Non-reactive products	Reactive products	Non-reactive products
Agilent 8800 ICP QQQ (Hogmalm et al., 2017)	*10%	90%	*85%	15%
Agilent 8900 ICP QQQ This project	**12%	88%	***99.85%	0.15%
Difference %	2%		14.85%	

Table 19: O_2 and N_2O standards $^{87}Sr/^{86}Sr$ ratios

Sample	QQQ $^{103}Sr/^{102}Sr$	Normalised	Recommended $^{87}Sr/^{86}Sr$	Normalisation factor	Deviation %
***n=1 O_2, n=10 N_2O**				O_2 $^{87}Sr/^{86}Sr$ ratios	
G-2	.714863 ± 0.0003	**.712719**	.709748 ± 2	1.003008	0.4186
GSP-2	.767411±0.0004	**.76555**	.765120 ± 2	1.007270	-0.4169
				N_2O $^{87}Sr/^{86}Sr$ ratios	
G-2		**.709915**	.709748 ±2	1.045458	0.0235
GSP-2		**.76493**	.765120 ± 2	1.045704	-0.0235

Table 20: Precision and accuracy of O_2 and N_2O $^{87}Sr/^{86}Sr$ ratios to recommended vaules

Sample	Recommended	Experiment 1 O_2		Experiment 2 N_2O		Experiment 4 N_2O	
	$^{87}Sr/^{86}Sr$	$^{87}Sr/^{86}Sr$	Deviation %	$^{87}Sr/^{86}Sr$	Deviation %	$^{87}Sr/^{86}Sr$	Deviation %
G-2	0.709748 ± 2	0.**7**14877	0.7226	0.**709725**	-0.0032	0.**709725**	-0.0032
GSP-2	0.765120 ± 2	0.**76**7450	0.3045	0.**765131**	0.0014	*0.**764720**	-0.0522

Numbers in bold indicate how close the experimental values for each experiment, within 4 decimal places to the recommended values to highlight the precision and accuracy of the reaction gases.
*In experiment 4 GSP-2 results are rounded up, would obtain three decimal places to recommended values

5.2. Concentration of Rb and Sr standards and rock samples

The standards G-2 and GSP-2 were used as reference materials for the measured concentrations of Rb and Sr using N_2O gas and solution-based analyses. The concentrations of Rb and Sr measured in the standards are within the errors or very close to recommended values (Table 21 and Figure 11). However, the concentrations of Rb and Sr measured in our rock samples (Table 17) deviate quite a lot if compared to concentrations published for the same rock types. This may suggest the samples analysed in this study may have been collected from slightly different locations or outcrops within the same rock types; also different methods were applied for this study and published studies to obtain Rb and Sr concentrations. Our excellent agreement of the Sr and Rb concentrations for G-2 and GSP-2 (measured with N_2O gas) confirms that the method and analytical setup used in this study is robust and accurate, and the observed discrepancies in the concentrations for rock samples are thus likely due to a natural variability in Sr and Rb contents in these different rock types.

Table 21: O_2 and N_2O comparison of Rb and Sr concentrations for standards

	Concentrations						
	Recommended	**Experiment 1 O_2**		**Experiment 2 N_2O**		**Experiment 4 N_2O**	
G-2			**Dev.%**		**Dev.%**		**Dev.%**
Rb ppm	168.5± 3	154.3	-8.4	165.6 ± 0.16	-1.7	173.5 ± 0.28	2.9
Sr ppm	474.9 ± 2	464.5	-4.8	466.6 ± 25.4	-1.7	483.7± 0.74	1.8
GSP-2							
Rb ppm	245 ± 7	245.3	-10.1	220.2 ± 0.39	0.1	249.7± 0.40	1.9
Sr ppm	240 ± 10	235.9	-0.8	238.7 ± 27.8	-0.5	243.9±0.36	1.6

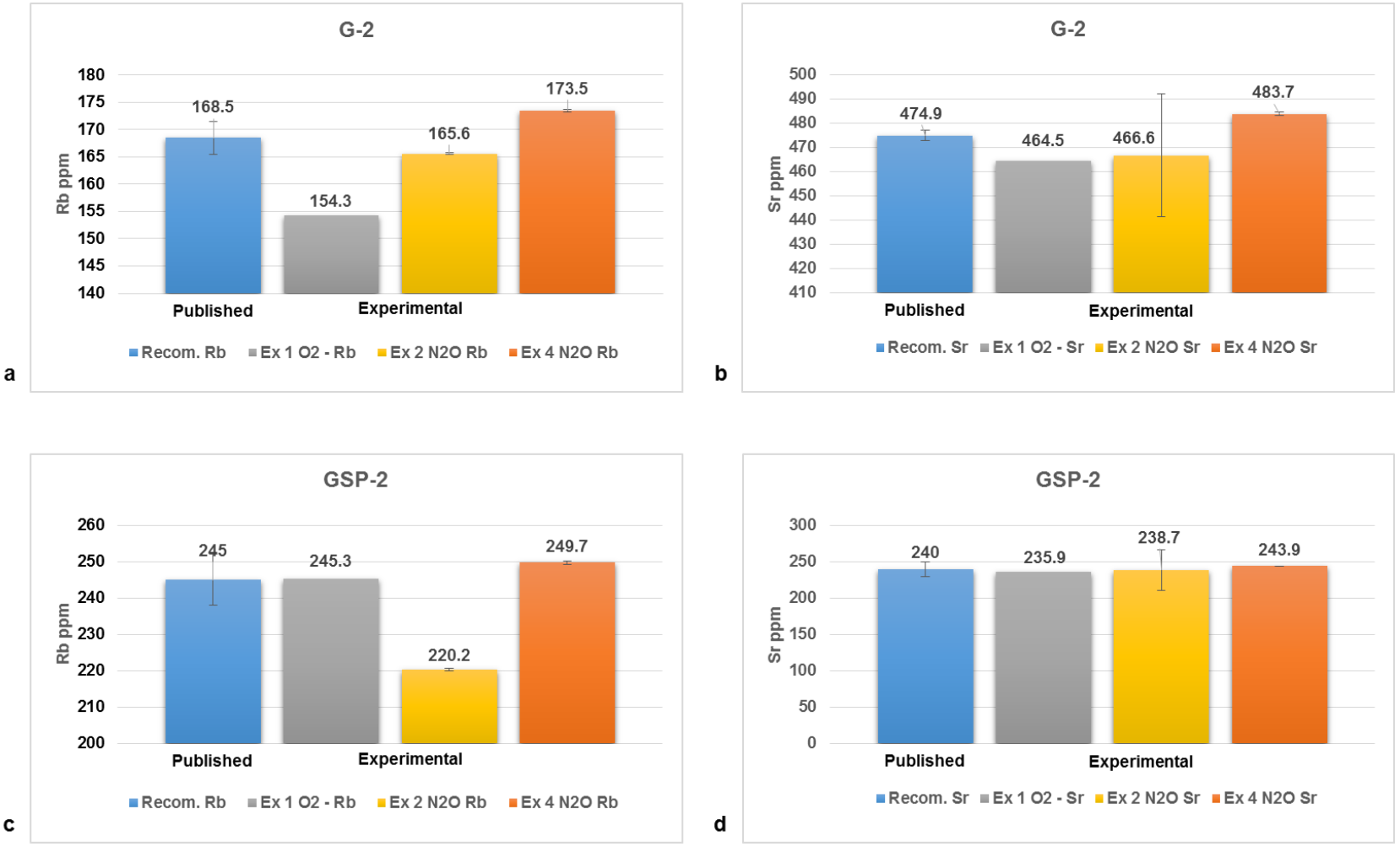

Figure 11: Comparison of concentrations to TIMS recommended values of standards a: G-2 Rb ppm, b: G-2 Sr ppm, c: GSP-2 Rb ppm, d: GSP-2 Sr ppm.

5.3. In-situ Rb-Sr dating

The acquired in-situ Rb-Sr ages of studied minerals and rocks are compared to the published ages (see Figure 12), as determined by various geochronological methods (for details see also information in Table 22). Specific ages for individual samples acquired by this study, and their comparisons to published results, are discussed in detail below.

5.3.1 LP-6

LP-6 biotite published age is 128.2±2.2 Ma with initial $^{87}Sr/^{86}Sr$ of 0.7130±0.0014 determined by Rb-Sr and K-Ar dating methods (Li et al., 2008). The in-situ Rb-Sr age acquired by this study for LP-6 is 127±12 Ma with different initial $^{87}Sr/^{86}Sr$ of 0.7201±0.0067 which is slightly higher than the published result. The possible cause for the slightly higher initial $^{87}Sr/^{86}Sr$ (although the difference is rather marginal considering the analytical errors) could be due to minor inhomogeneities in LP-6 mineral grains or batches. Overall, the age acquired by this study via LA-QQQ method agrees (within the error) with the published crystallisation age for LP-6 biotite. The rather large error for our in-situ Rb-Sr dating for LP-6 is related to younger age for this mineral, and the associated minor ingrowth of the radiogenic ^{87}Rb, which in turn causes limited variation and spread in $^{87}Sr/^{86}Sr$.

5.3.2 Padthaway Granite: PG-11

The biotite grains from the Padthaway Granite (PG-11 sample) were targeted within a section of whole rock sample for the in-situ Rb-Sr dating of PG-11. The published crystallisation age for the Padthaway Granite, dated by U-Pb method is reported to be 487.1±1.2 Ma (Foden et al., 2006). The results from in-situ Rb-Sr dating yielded an age of 479.4±9.4 Ma, which is thus within the error of the published age. The interpretation of the in-situ Rb-Sr age of PG-11 is that it reflects the crystallisation age of the rock.

Further support for this interpretation of primary ages comes from our observations of thin sections and minerals that show no obvious indices for secondary alterations, (based on Turner (1992) and Turner et al. (1992). This however, does not mean the rock was not subjected to some younger thermal event where the temperature could have risen considerably, but based on our results not above ~400°C, which is the closure temperature of the Rb-Sr system in biotite (Dodson, 1973).

5.3.3 Black Hill Gabbro: BHG-1

The biotite grains had been individually picked for in-situ Rb-Sr dating from the Black Hill Gabbro (i.e., sample BHG-1). The original method of dating was by Rb-Sr and K-Ar methods which reported the published age for Black Hill Gabbro of 487±5 Ma. The results from our in-situ Rb-Sr dating was 481.6±6 Ma, which thus shows excellent agreement with the published age. The interpretation of these concordant ages could indicate a metamorphic age of the rock as previously suggested in literature, based on the description of the minerals showing altered perthitic alkali feldspar, which indicates that Black Hill Gabbro had undergone thermal alteration during its history which may have reset the Rb-Sr isotope system within the rock.

5.3.4 Rathjen Gneiss: RG

The biotite for the Rathjen Gneiss (RG sample) was targeted within the whole rock for in-situ Rb-Sr dating. The original method of dating was by U-Pb and Rb-Sr methods with reported crystallisation age for the Rathjen Gneiss of about 514±5 Ma (Foden et al., 1999). The results from in-situ Rb-Sr dating of RG sample is 502.0±9.9 Ma, and thus within the error of the published age.

The above ages likely indicate the original metamorphic age of Rathjen Gneiss formations, based also on the visual observations of gneissic fabric and mineral alteration patterns in the thin sections (see also Foden et al. (1999).

Table 22: Published ages and in-situ Rb-Sr ages

Original Dating Methods				In-situ Rb-Sr dating LA-QQQ N_2O			
Sample		Published Age	Method	Sample	Age	Error	Initial $^{87}Sr/^{86}Sr$
LP-6	Biotite	128.2 ± 2.2 Ma (Li, Chen, Li, Wang, & He, 2008)	Rb-Sr K-Ar	Biotite	127 ± 12 Ma	9.4%	0.7201 ± 0.0067
Padthaway Granite PG-11	Zircon	487.1 ± 1.2 Ma (Foden, Elburg, Dougherty-Page, & Burtt, 2006)	U-Pb	Biotite in whole rock	479.4 ± 9.4 Ma	2.0%	0.7200 ± 0.0071
Black Hill Gabbro BHG-1	Whole rock & Biotite	487 ± 5 Ma (Milnes et al., 1977)	Rb-Sr K-Ar	Biotite	481.6 ± 6 Ma	1.2%	0.7202 ± 0.0070
Rathjen Gneiss RG	Zircon	514 ± 5 Ma (Foden et al., 1999)	U-Pb Rb-Sr	Biotite in whole rock	502.0 ± 9.9 Ma	2.0%	0.7199 ± 0.0071

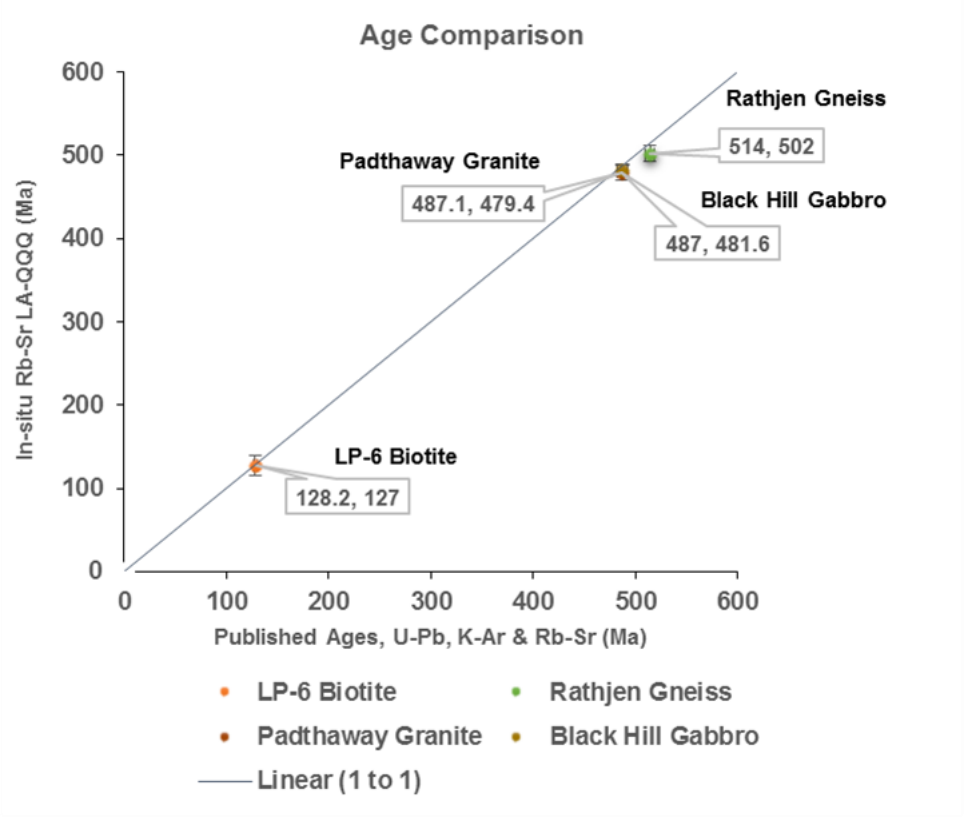

Figure 12: Published ages and In-situ Rb-Sr ages of studied rock types.
Published ages: LP-6 Biotite (Li et al., 2008), Padthaway Granite and Rathjen Gneiss (Foden et al., 2006), Black Hill Gabbro (Milnes et al., 1977).

6. CONCLUSION

- The tests conducted for this study had utilised N_2O gas in three experiments on Rb and Sr isotopes in mass-shift mode, which demonstrated to be an excellent reaction gas on the new Agilent 8900 ICP-QQQ, but also has been confirmed by earlier studies on the Agilent 8800 ICP-QQQ.
- There is a need to consider appropriate and consistent standards to be used for in-situ Rb-Sr dating method. For this study the ages were calculated using the average of two mica standard one older and the other younger in age (Mica-Mg and LP-6) for all samples, which has shown to work in this study on biotites for in-situ Rb-Sr dating to gain ages close to the published ages.
- The sensitivity gained by the new Agilent 8900 ICP-QQQ provides the robustness and reliability for Rb-Sr dating method when using highly reactive gases such as N_2O gas.
- This study has found the results produced by O_2 and N_2O gas by monitoring Sr^+ isotopes in on-mass and mass-shift mode (i.e., measuring the intensity of Sr^+ and SrO^+). The results for O_2 were 12% yield of SrO^+ reaction products whereas N_2O had a much larger yields of up to 99.85%, which indicates the suitability of N_2O gas for accurate and precise results for in-situ Rb-Sr dating method.
- The average error obtained from in-situ Rb-Sr isochrons ages was 1.7% from the rock samples, this shows the in-situ Rb-Sr dating method to be a successful tool to use for geochronology.
- The LA-QQQ approach has also potential for other beta decay dating methods such as ^{40}K-^{40}Ca dating method by Hogmalm et al. (2017), where removal of isobaric interferences is critical and could be performed in a reaction cell.

ACKNOWLEDGEMENTS

Thank you to Juraj Farkas for all your support and having faith in me to take on this project, it has been an amazing challenge. Co-supervisors Karin Barovich and Alan Collins for your contribution of editing this thesis and to John Foden, for providing the rock samples and mineral separates of known ages used for this project. A special thank you to Ahmad Redaa PhD Candidate, for your support, assisting with preparation and during the experiments. Technical expertise and support of Sarah Gilbert at Adelaide Microscopy was commendable during experiments conducted on Agilent 8900 ICP-QQQ and setting up the LA-QQQ. Agilent Technologies for funding the experiments; Fred Fryer your time and expert knowledge of the Agilent 8900 ICP-QQQ; Caroline Forbes for supplying technical resources and table of relative isotopic abundance. Thomas Zack, University of Gothenburg for joining the experiment LA-QQQ in-situ Rb-Sr dating, expert knowledge and the use of special nano-powder standards was greatly appreciated. Thanks to the honour students who have helped throughout the year. To my supportive and understanding family, thank you. This thesis is dedicated in memory of my father.

REFERENCES

BANDURA, D., BARANOV, V., & TANNER, S. (2001). Reaction chemistry and collisional processes in multipole devices for resolving isobaric interferences in ICP–MS. *Fresenius' journal of analytical chemistry, 370*(5), 454-470.

BOLEA-FERNANDEZ, E., BALCAEN, L., RESANO, M., & VANHAECKE, F. (2016). Tandem ICP-mass spectrometry for Sr isotopic analysis without prior Rb/Sr separation. *Journal of Analytical Atomic Spectrometry, 31*(1), 303-310.

BOLEA-FERNANDEZ, E., BALCAEN, L., RESANO, M., & VANHAECKE, F. (2017). Overcoming spectral overlap via inductively coupled plasma-tandem mass spectrometry (ICP-MS/MS). A tutorial review. *Journal of Analytical Atomic Spectrometry*.

COMPSTON, W., CRAWFORD, A., & BOFINGER, V. (1966). A radiometric estimate of the duration of sedimentation in the Adelaide Geosyncline, South Australia. *Journal of the Geological Society of Australia, 13*(1), 229-276.

DODSON, M. H. (1973). Closure Temperature in Cooling Geochronological and Petrological Systems *Contr. Mineral, and Petrol, 40*, 259-274.

FODEN, J., ELBURG, M., DOUGHERTY-PAGE, J., & BURTT, A. (2006). The timing and duration of the Delamerian Orogeny: correlation with the Ross Orogen and implications for Gondwana assembly. *The Journal of Geology, 114*(2), 189-210.

FODEN, J., ELBURG, M., TURNER, S., SANDIFORD, M., O'CALLAGHAN, J., & MITCHELL, S. (2002). Granite production in the Delamerian orogen, South Australia: Journal of the Geological Society of London, v. 159. *doi, 10*, 0016-764901.

FODEN, J., SANDIFORD, M., DOUGHERTY-PAGE, J., & WILLIAMS, I. (1999). Geochemistry and geochronology of the Rathjen Gneiss: implications for the early tectonic evolution of the Delamerian Orogen. *Australian Journal of Earth Sciences, 46*(3), 377-389.

FODEN, J., SONG, S., TURNER, S., ELBURG, M., SMITH, P., VAN DER STELDT, B., & VAN PENGLIS, D. (2002). Geochemical evolution of lithospheric mantle beneath SE South Australia. *Chemical Geology, 182*(2-4), 663-695. doi: Doi 10.1016/S0009-2541(01)00347-3

GOVINDARAJU, K. (1979). Report (1968–1978) on Two Mica Reference Samples: Biotite Mica-Fe and Phlogopite Mica-Mg. *Geostandards and Geoanalytical Research, 3*(1), 3-24.

GOVINDARAJU, K. (1994). 1994 compilation of working values and sample description for 383 geostandards. *Geostandards and Geoanalytical Research, 18*(S1), 1-158.

HOGMALM, K., ZACK, T., KARLSSON, A.-O., SJÖQVIST, A., & GARBE-SCHÖNBERG, D. (2017). In situ Rb–Sr and K–Ca dating by LA-ICP-MS/MS: an evaluation of N 2 O and SF 6 as reaction gases. *Journal of Analytical Atomic Spectrometry, 32*(2), 305-313.

LI, Q., CHEN, F., LI, X., WANG, F., & HE, H. (2008). Single grain Rb-Sr isotopic analysis of GA-1550 biotite, LP-6 biotite and Bern-4M muscovite 40Ar-39Ar dating standards. *Geochemical Journal, 42*(3), 263-271.

LUDWIG, K. (Revised 2009). Isoplot (Version 4.15): Berkeley Geochron Centre. Retrieved from http://www.bgc.org/isoplot_etc/isoplot.html

MILNES, A., COMPSTON, W., & DAILY, B. (1977). Pre-to syn-tectonic emplacement of early Palaeozoic granites in southeastern South Australia. *Journal of the Geological Society of Australia, 24*(1-2), 87-106.

PERKINS, D., HENKE, K.R. (2004). *Minerals in Thin Section* (2nd ed.). Upper Saddle River, New Jersey: Pearson Education, Inc.

QUANSYS-BIOSCIENCES. (2005). Dilutions: Explanations and Examples of Common Methods. Retrieved from http://www.quansysbio.com/dilutions/

TECHNOLOGIES, A. (2016). Agilent 8900 Triple Quadrupole ICP-MS Technical Overview. *Agilent Technologies*, (5991-6990EN), 1-10.

TURNER, S. (1992). *Late-orogenic, Mantle-derived, Bimodal Magmatism in the Southern Adelaide Foldbelt, South Australia*: University of Adelaide, Department of Geology and Geophysics.

TURNER, S. (1996). Petrogenesis of the late-Delamerian gabbroic complex at Black Hill, South Australia: implications for convective thinning of the lithospheric mantle. *Mineralogy and Petrology, 56*(1-2), 51-89.

TURNER, S., & FODEN, J. (1996). Magma mingling in late-Delamerian A-type granites at Mannum, South Australia. *Mineralogy and Petrology, 56*(3-4), 147-169.

TURNER, S., FODEN, J., & MORRISON, R. (1992). Derivation of some A-type magmas by fractionation of basaltic magma: an example from the Padthaway Ridge, South Australia. *Lithos, 28*(2), 151-179.

VILLA, I., DE BIÈVRE, P., HOLDEN, N., & RENNE, P. (2015). IUPAC-IUGS recommendation on the half life of 87 Rb. *Geochimica et cosmochimica acta, 164*, 382-385.

WISE, S. A. (2007). Standard Reference Material 987 - Strontium Carbonate (Isotopic Standard). *Certificate of Analysis*, 1-2.

ZACK, T., & HOGMALM, K. (2016). Laser ablation Rb/Sr dating by online chemical separation of Rb and Sr in an oxygen-filled reaction cell. *Chemical Geology, 437*, 120-133.

APPENDICES

Appendix 1: Method - cleaning vial and bomb procedures

Rigorous processes were conducted for cleaning of vials and bombs:

- Polypropylene vials of 200 ml, 50 ml, 20 ml and 5 ml were cleaned in the Easy Trace Cleaner (ETC) in three stages using 12M (molar) (37%) HCl, deionised water (DI) water and heating to 140°C.
- Teflonwear had undergone a pre-cleaning process prior to cleaning: vials ten 15 ml and 7 ml had 6M HCl, DI water and heating to 140°C; seven bombs 23 ml, had 6M HCl, DI water and heating to 100-250°C. There are five stages for cleaning teflonware. All were placed in the ETC with 15M (70%) HNO_3, DI water, 12M (37%) HCl and HF acids heating to 170°C.
- Sarstedt vials of 50 ml were cleaned in two stages with HCl and DI water heated to 80°C.

Polypropylene (plastic) vials (experiment 1 & 2)

Place polypropylene vials of 200 ml, 50 ml, 20 ml and 5 ml with lids in upper half and vials in lower half into the Easy Trace Cleaner (ETC). Three stages of cleaning:

Stage 1: 700 ml of 12M (37%) HCl into (ETC), heat to 140°C for 24 hours and label signage card of process (name, phone, date and tick HCl); empty ETC of used HCl into waste bottle.

Stage 2: 700 ml of deionised (DI) water into ETC, heat to 140°C for 24 hours and label signage card of process (tick DI water); empty ETC of used DI water.

Stage 3: Plastic lids and vials facing up on hotplate at 90°C for 1 hour to dry.

Teflownwear (experiment 4)

Pre-cleaning: wipe off previous labels from lid and vial with ethanol or acetone.

Vials of 15 ml and 7 ml cleaned: pour 1-2 ml of recycled 6M HCl into each vial, recap and onto hotplate at 140°C in fume cupboard for ~30 minutes; take off hotplate to cool; uncap vials, pour out waste HCl acid into container; empty vials in a large beaker of DI water.

Bombs of 23 ml cleaned: place bombs in 3 L glass beaker to maximum half-full; 6M HCl into beaker covering bombs; glass lid to cover and pour DI water on lid (to help condense HCl vapours); onto hotplate to ~100-250°C in fume cupboard for ~3-4 hours (to dissolve external corrosion deposits from previous use); allow to cool; drain remaining DI water from glass lid; wearing safety apron and gloves, drain the 6M HCl into used acid container and empty the remaining acid in bombs. The five stages of cleaning:

Stage 1: Load pre-cleaned bombs and vials into ETC, placing vials on lower half and lids on upper half; cover ETC and pour through top feed funnel ~700 ml 15M (70%) HNO_3 and replace stopper; place in fume cupboard on hotplate at 170°C, label signage card of process (name, phone, date and tick HNO_3) heat for 48 hours; drain used HNO_3 acid and close stopcock, when acid has cooled, place in original bottle.

Stage 2: ~700 ml DI water and replace stopper; repeat stage 1 (tick DI water) heat for 24 hours; when cooled pour DI water down drain.

Stage 3: ~700 ml 12M (37%) HCl; repeat stage 1 (tick HCl) for 48 hours; the used HCl acid when cooled in original bottle.

Stage 4: Repeat stage 2; when cool remove without touching the inside lip of the vials and lids.

Stage 5: Involves the use of HF, caution: safety equipment must be worn and dispensed in the fume cupboard; tefloneware vials add ~5 ml single distilled 7M HNO_3 with ~5 ml single distilled (10-20%) 28M HF into each vial; recap vials and onto hotplate at 140°C, repeat stage 1 (tick HNO_3 + HF) heat for 12 hours; after 12 hours cool vials and pour out used acid into the waste container; any residual acid place vials onto hotplate to evaporate acid; place into storage container for use.

Sarstedt plastic vials (experiment 4)

These vials are cleaned differently to the other vials, this is due to text on exterior of vials. The two stages of cleaning:

Stage 1: ~5 ml of HCl into Sarstedt plastic vials (50 ml), recap vials, onto the hotplate at 80°C for overnight; uncap lid to evaporate acid on hotplate at same temperature.

Stage 2: Squirt ~2 ml of DI water and place on hotplate to dry.

Appendix 2: Method - dilution approach for solutions

Dilution method for calculating concentration and dilutions of solutions the formula used was Quansys-Biosciences (2005), $C_1V_1 = C_2V_2$ where:

- V_1 = volume of stock solution required for new solution
- C_1 = concentration of stock solution
- V_2 = final volume of new solution
- C_2 = final concentration of new solution

Formula $V1 = \frac{C2V2}{C1}$

Three stage dilution using Equation 1 (Appendix 6):

Stage 1: 150 ml solution of Rb and Sr in 200 ml plastic vial; 147 ml HNO_3 + 3 ml 10 µg/mL High Purity Standard of Rb or Sr isotope solution to produce concentration of 200 ppb in for both solutions (Table 23)

Stage 2: Prescribed ml of HNO_3 from Table 23 with 1ml or 5ml pipettes into 200 ppb of Rb or Sr solutions to produce mixes 50 ml vials of final solution with new concentrations of 100 ppb, 40 ppb, 20 ppb and 10 ppb (Table 24)

Stage 3: From Stage 2 using Table 23 take various concentrations to make up Rb-Sr mix dilutions in 50 ml vials: 25 ml 200 ppb Rb + 25 ml 200 ppb Sr solutions to produce mixtures of 100 ppb, 50 ppb, 20 ppb and 10 ppb (Table 25).

Table 23: Stage 1 – preparation steps for Rb and Sr isotope solutions

Required Concentrations	Original solution		Required volume and concentrations		Preparation steps		Final Solutions	
					Isotope	Acide HNO_3		
10000 ppb	V1	C1 ppb	V2 ml	C2 ppb	ml (V1)	ml	ml	ppb
200ppb		10000	150	200	3	147	150	200
100ppb		200	50	100	25	25	50	100
40ppb		200	50	40	10	40	50	40
20ppb		200	50	20	5	45	50	20
10ppb		200	50	10	2.5	47.5	50	10

Table 24: Stage 2 – new concentrations of Rb and Sr isotope solutions

Required Concentrations	Original solution		Required volume and concentrations		New volume	New concentration
Strontium	Isotope V1	Isotope C1 ppb	Acide HNO_3 V2	C2 ppb	g	ppb
200 ppb	3.04463	10000	144.88124	200	147.92587	205.82133
100 ppb	24.89439	205.82133	24.71835	100	49.61274	103.27582
40 ppb	10.10784	205.82133	39.79746	40	49.90530	41.68714
20 ppb	5.30807	205.82133	44.61930	20	49.92737	21.88207
10 ppb	2.53152	205.82133	47.61255	10	50.14407	10.39088

Table 25: Stage 3 – Rb-Sr mixed solutions

Required Concentrations	Rubidium Solution		Strontium Solution		Final Mixed Solutions		
Rb-Sr mix	V1 g	Rb C1 ppb	Sr V2 g	Sr C2 ppb	V g	Rb ppb	Sr ppb
mix 100 ppb	24.52394	201.75985	24.54863	205.82133	49.07257	100.82917	102.96245
mix 50 ppb	25.16424	99.85180	24.60738	103.27582	49.77162	50.48449	51.06017
mix 20 ppb	24.15264	39.18139	24.64241	41.68714	48.79505	19.39406	21.05278
mix 10 ppb	24.52660	20.67347	24.80294	21.88207	49.32954	10.27883	11.00232

Appendix 3: Method - dilution of standards for experiment 1 (O_2) and experiment 2 (N_2O)

The rock standards G-2 and GSP-2 were prepared by the Clean Laboratory Technician. Recommended values from the USGS certificates' of G-2 and GSP-2 for Rb and Sr elements were used to calculate concentrations and volume in two stages and SRM 987 Sr in second stage. The solution of these three standards were used in Experiments 1 and 2.

Stage 1: ~0.1 g using metal of dissolved rock standards and add 10 ml of HNO_3 to make concentrated standard solution (Table 26).

Stage 2: 2 ml of the concentrated standard solution and dilute with 18 ml HNO_3 to make 20 ml solution (Table 27).

Table 26: Stage 1 – preparation for dilution of standards

Initial concentration			Concentration		Add	Result 1:100	
Element	ppm	±	ppm	V1 (g)	HNO_3 g	C2 ppb	V2 (ml)
G-2							
Rb	170	3	17.2312	0.10136	10.07461	171.635179	10.17597
Sr	478	2	48.45008	0.10136	10.07461	482.5977385	10.17597
GSP-2							
Rb	245	7	24.94345	0.10181	9.9801	251.8861	10.08191
Sr	240	10	24.4344	0.10181	9.9801	246.7455	10.08191

Table 27: Stage 2 – final dilution of standards

	Stage 2		Add	Final Result 1:1000	
Element	C1 ppm	V1 (ml)	HNO_3 g	C ppb	V2 (ml)
G-2					
Rb	172.9029	2.04491	17.99636	17.64214	20.04127
Sr	486.1623	2.04491	17.99636	49.60554	20.04127
GSP-2					
Rb	251.8861	1.96858	17.42454	25.56875	19.39312
Sr	246.7455	1.96858	17.42454	25.04694	19.39312
NIST SRM 987					
Sr	1000	0.0008	17.53472	45.62169	17.53552

Appendix 4: Method - dissolving standards, rock powders and mineral separates

The preparation of samples to be dissolved for Experiment 4 is to extract Rb and Sr, through online separation for isotopic analysis on the Agilent 8900 ICP-QQQ. The samples were taken from whole rock powders of the two standards: G-2 and GSP-2, and three samples: RG, PG-11 and BHG-1 and mineral separates of LP-6 (standard) and one sample BHG-1 biotite Agilent 8900 ICP-QQQ. All five-rock powders were dissolved in a pressure digestion vessel (bomb) under high pressure and temperature to dissolve any resistant minerals that maybe present within the whole rock standards and samples. The two biotites were dissolved in teflonware vials. Included two blanks: one bomb and one teflonware vial, which had undergone the same dilution procedures as the samples for quality control. There are 5 stages for dissolving standards and sample rock powders and biotite grains.

Stage 1: ~0.1 g of the two standards G-2 and GSP-2, and three whole rock sample powders RG, PG-11 and BHG-1, and one biotite (BHG-1) mineral separate, and 0.2 g of standard LP-6 biotite (Table 28) into bombs and vials.

Stage 2: 2 ml 7M HNO_3 and 4 ml HF; place on hotplate 140°C with lids off to evaporate acid, ~2 hours; before complete evaporation squirt small amount of 15M HNO_3 then evaporate completely, ~30 minutes; take off hotplate; repeat same above measurement of initial acids for both bombs and vials.

Stage 3: a) vials: lids on vials, place on hotplate at 140°C for 2 days;

b) bombs: carefully transported (contains HF) to another lab with oven; prepare metallic casings for teflon bombs with 'Dry Glide' spray on screw thread (for ease of screwing lid off), place bombs in metallic casing, screw lids on, place in oven for 4 days at 150°C.

Stage 4: a) vials: on 3rd day cool, tap base of vials to knock off condensation from lid; with lid off place on hotplate on 140°C to evaporate the acids again before total evaporation add a squirt of 15M HNO_3;

b) bombs: on 5th day take bombs out of oven and cool in metallic bombs, take Teflon bombs out of metallic bombs and transport back to clean lab carefully (still contains HF); take bomb lids off, place on hotplate 140°C to evaporate the acids, again before total evaporation add a squirt of 15M HNO_3;

Stage 5: a) vials: measure 6 ml of 6M HCl, with lid on vial, repeat stage 3a for 1 day.

b) bombs: measure 8 ml of 6M HCl, repeat stage 3b for 1 day.
All stages completed for standards and samples ready for dilution process.

Table 28: Stage 1 – preparation for dissolving standards, rock samples and mineral separates

Sample	0.1 g
44 Bomb - Blank	0
35 - G-2	0.0996
24 - GSP-2	0.1091
14 - BHG-1	0.1747
9 - RG	0.1059
43 - PG-11	0.1136
2321 vial - Blank	0
BHG-1 - Biotite	0.1068
	0.2 g
LP-6 - Biotite	0.19149

The table above shows how much rock powder was measured from each sample when weighed on the scales.

Appendix 5: Method - dilution of standards and samples for experiment 4 (N_2O)

The tables below express the steps of dilution that occurred for the experiment preparation:

- Step 1 dilution (1/10) was calculated from V1g/V2ml in Table 29
- Step 2a dilution (1/100) was calculated from V1/V2 in Table 30
- Step 2b dilution (1/10000) was calculated from dilution 1/dilution 2 in Table 30
- Step 3 final dilution calculated from 1/dilution 3 in Table 31.

Table 29: Step 1 dilution (1:10)

Samples	Sample dilution			Step 1 - 1:10	
	Powder 0.1 g (V1)	0.01 mg/g C1 ppm	V1 ml	Add 10 ml HNO_3 (V2)	C2 ppm
44 Bomb - Blank				9.87218	
35 - G-2	0.0996	47000		9.61354	486.938214
24 - GSP-2	0.1091	24000		10.21486	256.332441
14 - BHG-1 WR	0.1747			10.25135	
9 - RG - WR	0.1059			10.25211	
43 - PG-11 WR	0.1136			10.05762	
BHG-1 - Biotite	0.1068			10.08392	
LP-6 - Biotite	0.19149			20.43395	
2321 vial - Blank				10.15099	

Table 30: Step 2a and 2b dilution (1:100)

Samples	Step 2 1:100					
	C1 ppm	V1 ml	Add 39.6 ml HNO_3	V2 (ml)	C2 ppm	ppb
44 Bomb - Blank		0.40924	39.91369	40.32293		
35 - G-2	486.938214	0.411032	40.424178	40.83521	4.901339	4901.339
24 - GSP-2	256.332441	0.4018	39.75027	40.15207	2.565107	2565.107
14 - BHG-1 WR		0.41419	40.48211	40.8963		
9 - RG - WR		0.40459	40.13593	40.54052		
43 - PG-11 WR		0.4018	39.75027	40.15207		
BHG-1 - Biotite		0.40169	40.82356	41.22525		
LP-6 - Biotite		0.40405	39.9826	40.38665		
2321 vial - Blank		0.40692	40.10979	40.51671		

Table 31: Step 3 final dilution factor

	Dilution Factor			
Samples	**Dilution 1 1/10x**	**Dilution 2 1/100x**	**Dilution 3 1/10000x**	**Final Dilution**
44 Bomb - Blank				
35 - G-2	0.010360388	0.010065627	0.000104284	9589.217258
24 - GSP-2	0.010680518	0.010006956	0.000106879	9356.333113
14 - BHG-1 WR	0.017041658	0.010127811	0.000172595	5793.920944
9 - RG - WR	0.010329581	0.009979892	0.000103088	9700.440759
43 - PG-11 WR	0.011294919	0.010006956	0.000113028	8847.384443
BHG-1 - Biotite	0.010591119	0.009743786	0.000103198	9690.148145
LP-6 - Biotite	0.009371169	0.010004544	9.37543E-05	10666.18094
2321 vial - Blank		0.010043264		

Appendix 6: Method - equations

- Equation 1: dilution factors:

  $\frac{.1g\ (sample)}{10ml(HNO3)}$ = 1st dilution factor

  $V1\ x\ V2$ = 2nd dilution factor

  $1st\ dilution\ x\ 2nd\ dilution$ = 3rd dilution factor

  $3rd\ \frac{dilution}{1}$ = final dilution factor

- Equation 2: concentration factor for Rb and Sr

  $Sr\ dilution\ factor\ ppb\ x\ ^{104}Sr\ QQQ\ raw\ con\ ppb = {}^{88}Sr\ real\ con\ ppb$

  $\frac{^{88}Sr\ real\ con\ ppb}{1000} = ppm$

- Equations used for Experiment 1 to correct instrument drift of O_2 gas is found in Bolea-Fernandez et al. (2016) paper

- Equation 3: reaction products of O_2 and N_2O (raw data counts per second (CPS)

  $^{88}Sr\ CPS + {}^{104}Sr\ CPS = Total\ CPS$

  $^{88\ or\ 104}Sr + \frac{100}{Total\ CPS} = {}^{88\ or\ 104}Sr\ reaction\ products$

- Equation 4: $^{87}Sr/^{86}Sr$ ratios

  $\frac{measured\left(\frac{^{103}Sr}{^{102}Sr}\right)}{recommended\left(\frac{^{87}Sr}{^{86}Sr}\right)} = correction\ factor$

  $measured\ unknown\left(\frac{^{103}Sr}{^{102}Sr}\right)/standard\ correction\ factor\left(\frac{^{87}Sr}{^{86}Sr}\right)$ = $^{87}Sr/^{86}Sr$ ratio

- Equation 5: geochoronometry equation was rearranged to find LP-6 Biotite $^{87}Rb/^{86}Sr$ ratio:

  $\frac{^{87}Sr}{^{86}Sr} = \left(\frac{^{87}Sr}{^{86}Sr_0}\right) + \frac{^{87}Rb}{^{86}Sr}(e^{\lambda t} - 1)$

  Calculating $^{87}Rb/^{86}Sr$ ratio equation

  $\left(\frac{^{87}Rb}{^{86}Sr}\right) measured = \frac{\left(\frac{^{87}Sr}{^{86}Sr}\right) measured \left(\frac{^{87}Sr}{^{86}Sr}\right) initial}{(e^{\lambda t} - 1)}$

Appendix 7: Flowchart 2 - preparation sequence for solution work and laser

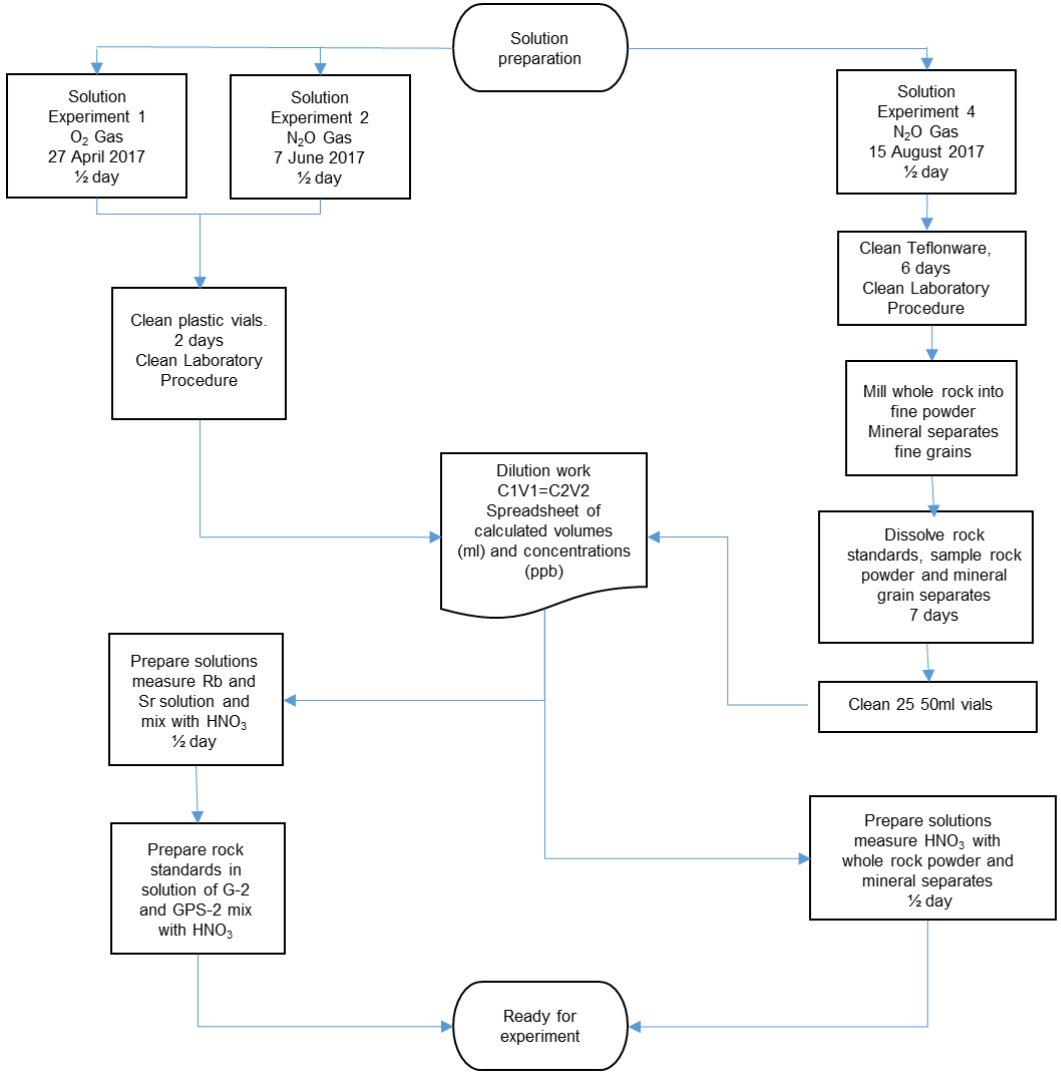

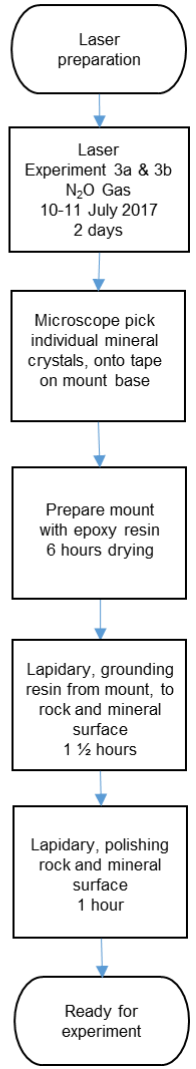

Appendix 8: Flowchart 3 - experiment design 1 and 2 – solution work

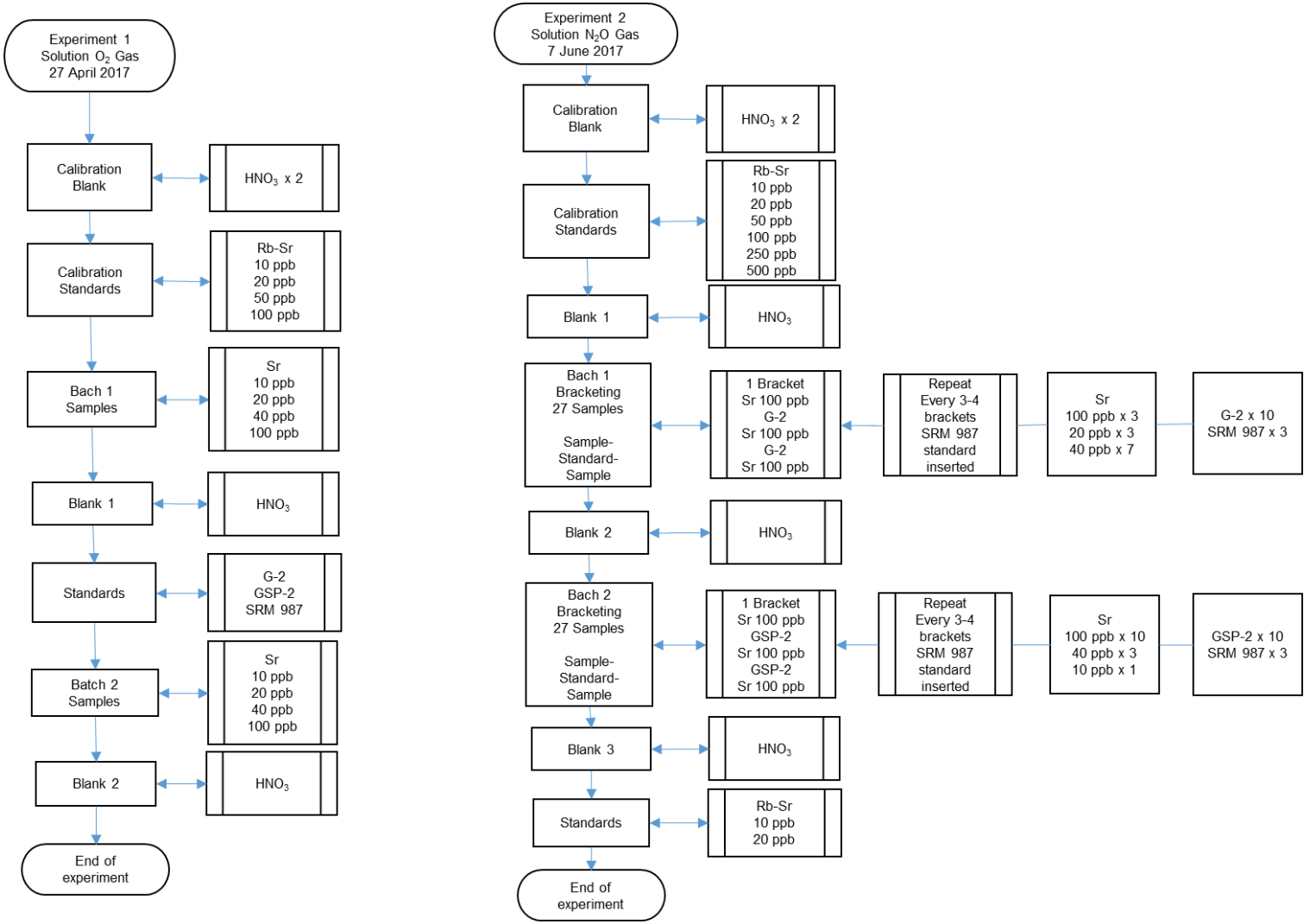

Appendix 9: Flowchart 4 - experiment design 4 – solution work

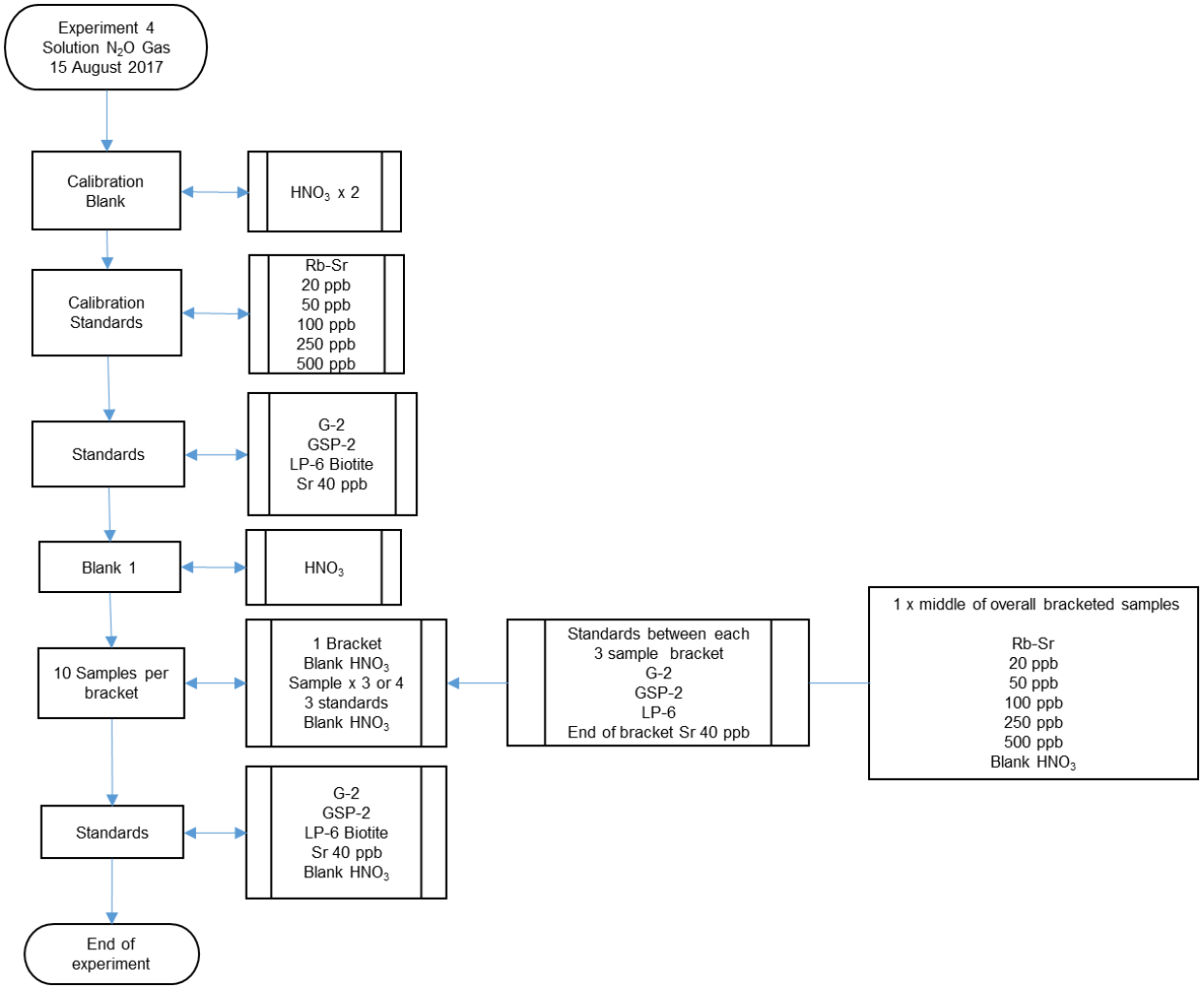

Appendix 10: Adelaide Microscopy – ICP-QQQ solution work

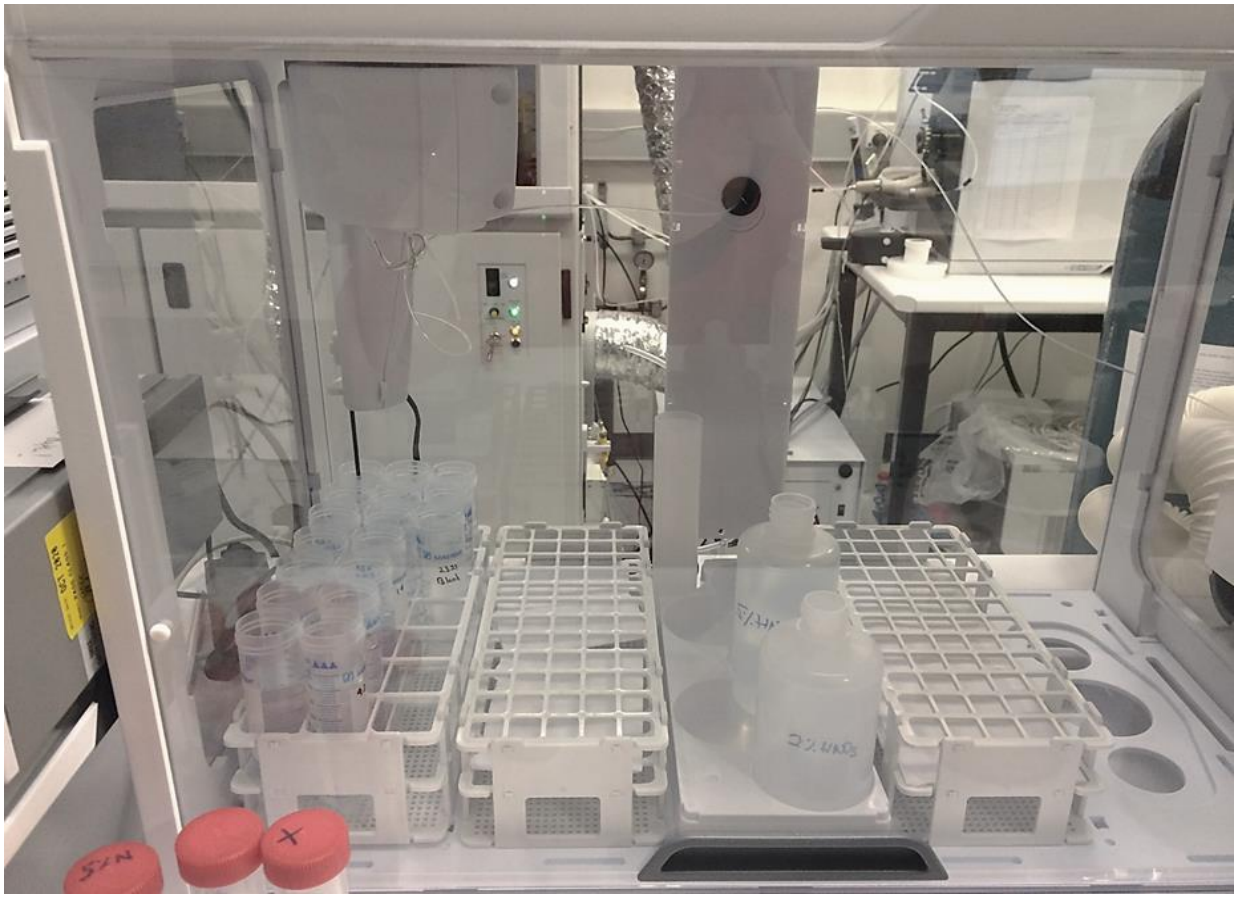

Appendix 11: Flowchart 5 - experiment design 3 – laser ablation

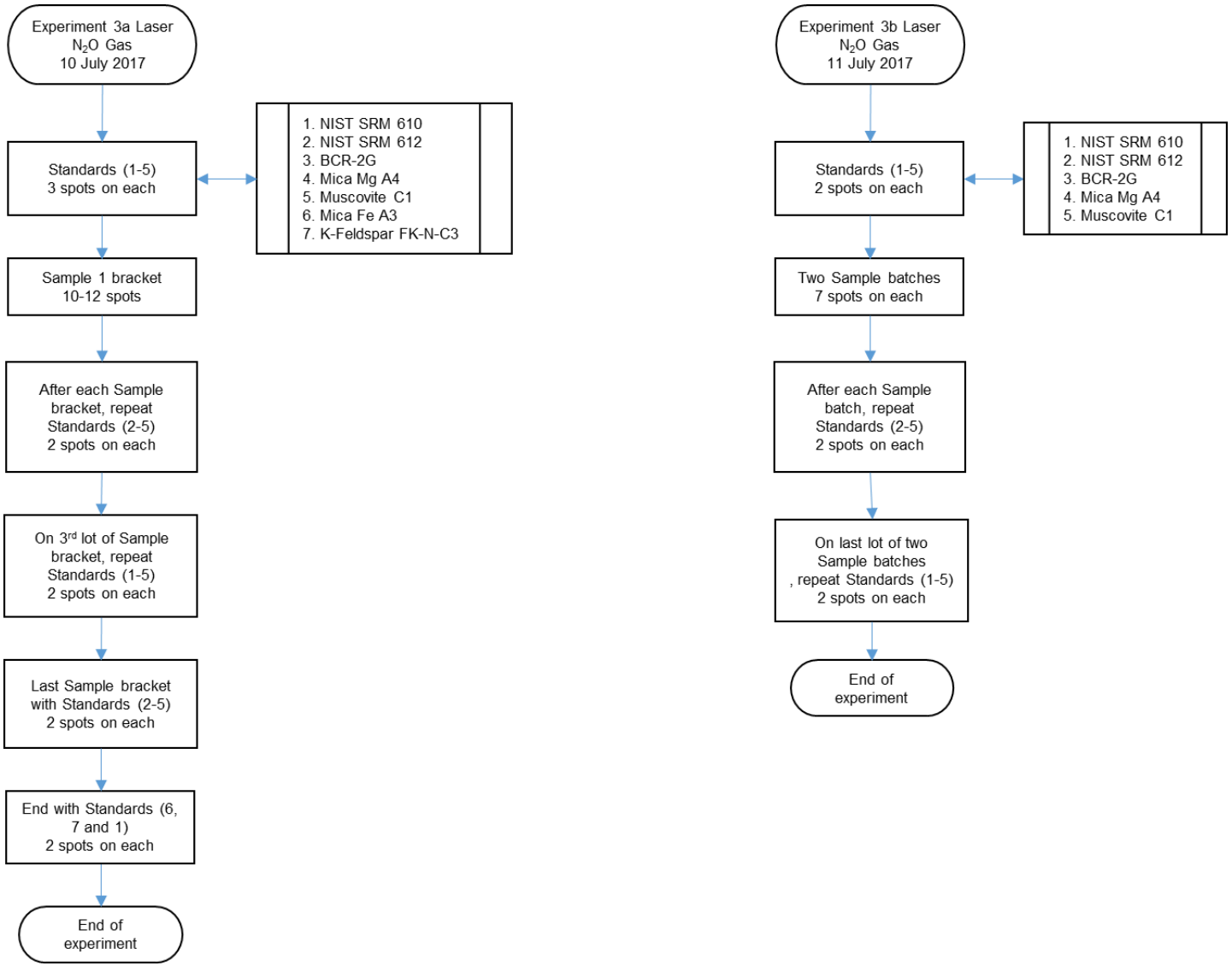

Appendix 12: Method – Lapidary of mounts

Polishing of mounts

Equipment used for polishing the mounts: Kunth Rotor lap (1st) using Struers Silicon Carbide paper of 1000 µm and 2000 µm and Kemet Diamond lap (2nd) using first the Blue cloth – fine (3 µm) with green diamond paste, then Brown cloth – very fine (1 µm) with blue diamond paste, located in the Rock Preparation Facility, Mawson building, University of Adelaide.

Step 3: Mounts out of moulds and discard double sided tape; using the 1st lap with continuous low flowing of water with 2000 µm or 1000 µm paper, grind the Epoxy mount gradually, checking every so often under the microscope to ground away epoxy to reveal surface of the rock or mineral grains, polish on the 2nd lap first using the blue cloth with green diamond paste, then repeat process with brown cloth with blue diamond paste, taking care not to over polish any biotite grains.

Appendix 13: Laser ablation set-up LA-QQQ

Key
A.R. – Ahmad Reda
B.A. – Brandon Alessio
L.J. – Lise Jensen
T.Z. – Thomas Zack
J.F. – Juraj Farkas
A.M – Adelaide Microscopy
St – Standard
KW – Kawr Suite (Saudi Arabia)
BHG – Black Hill Gabbro (SA)
RG – Rathjen Gneiss (SA)
PG-11 – Padthway Granite (SA)
HVQ – Heavitree Quartzite (NT)

A.M. Glass Standards
NIST SRM 610 Not used
NIST SRM 612 NIST SRM 614

A.M. Rock Standards
BCR-2G – Basalt Not used
GSD-1G
BHVO-2G

Laser set up for QQQ ICP-MS 10/07/2017

Appendix 14: Glitter reduction from laser ablation

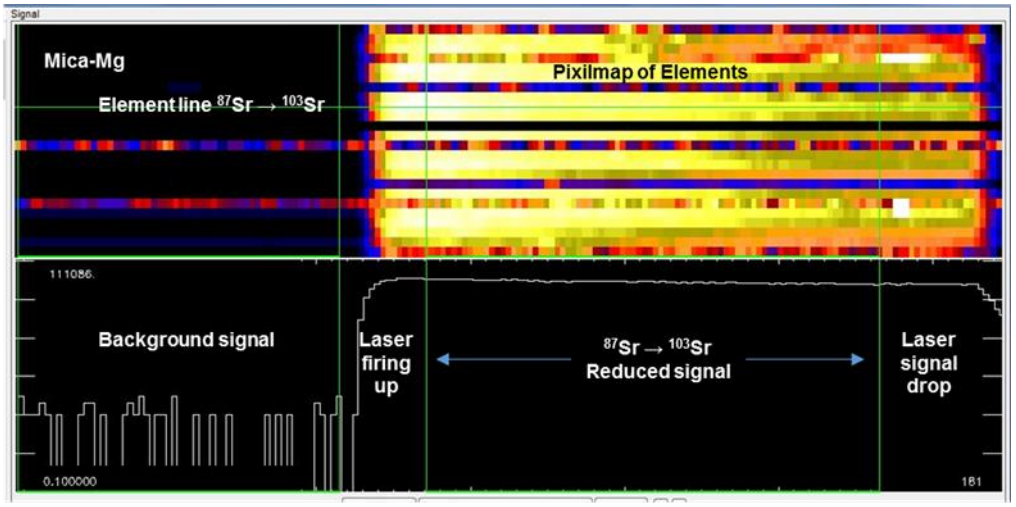

a

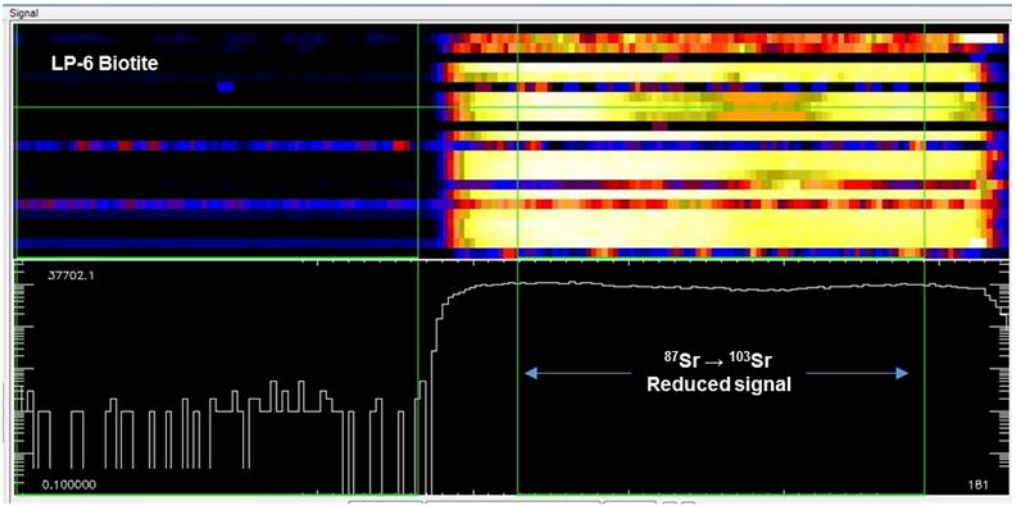

b

Appendix 15: Adelaide Microscopy - ASI RESOlution ArF excimer laser ablation system